

On-Shell Methods in Perturbative QCD

Zvi Bern,^{a,1} Lance J. Dixon^{b,2} and David A. Kosower^{c,3}

^a*Department of Physics and Astronomy, UCLA, Los Angeles, CA 90095-1547, USA*

^b*Stanford Linear Accelerator Center, Stanford University, Stanford, CA 94309, USA*

^c*Service de Physique Théorique, CEA-Saclay, F-91191 Gif-sur-Yvette cedex, France*

Abstract

We review on-shell methods for computing multi-parton scattering amplitudes in perturbative QCD, utilizing their unitarity and factorization properties. We focus on aspects which are useful for the construction of one-loop amplitudes needed for phenomenological studies at the Large Hadron Collider.

Key words:

PACS: 11.15.Bt, 11.25.Db, 11.55.Bq, 12.38.Bx

1. Introduction

The Large Hadron Collider (LHC) is poised to begin exploration of the multi-TeV energy frontier within the next year. It is widely anticipated that physics beyond the Standard Model will emerge at this scale, most likely via the production of new, heavy particles which may be associated with the mechanism of electroweak symmetry breaking. At the very least, the scalar Higgs boson of the Standard Model awaits discovery. New, heavy particles typically will decay rapidly into the known leptons, neutrinos, quarks and gluons. When the new physics model includes a dark matter candidate (as in supersymmetric models with conserved R parity), this particle can terminate the decay chain. In this case, sharp peaks in invariant-mass distributions may be scarce; they can be replaced by missing-energy signals. Quite often then, the signals for new physics have to be assessed against a significant background of Standard Model physics. The better

¹ Supported by the US Department of Energy under contract DE-FG03-91ER40662

² Supported by the US Department of Energy under contract DE-AC02-76SF00515

³ Laboratory of the *Direction des Sciences de la Matière* of the *Commissariat à l'Energie Atomique* of France

the background is understood, the better the prospects for discovery. Once new physics is discovered, we will want to measure its properties precisely, via production cross sections, branching ratios and masses. A numerically precise understanding of the backgrounds and of theoretical aspects of luminosity measurement will be essential to this endeavor.

In some cases backgrounds can be understood without much theoretical input. For example, in the decay of a light Higgs boson to a pair of photons, the signal is a very narrow peak in the di-photon invariant mass. The QCD background, in contrast, is a smooth distribution which can be interpolated easily under a candidate peak. However, many signals involve much broader kinematic distributions, with final states including jets and missing energy in addition to charged leptons and photons. A classic example is the production of a Higgs boson in association with a W boson at the Tevatron, with the Higgs decaying to a $b\bar{b}$ pair, and the W decaying to a charged lepton plus a neutrino. For such signals, a much more detailed understanding of the backgrounds is typically required.

Many methods are available for computing Standard Model backgrounds at the leading order (LO) in QCD perturbation theory. For example, MADGRAPH [1], CompHEP [2] and AMEGIC++ [3] automatically sum tree-level Feynman graphs for helicity amplitudes. Other programs, such as ALPGEN [4] and HELAC [5] are based on ‘off-shell’ recursive algorithms [6,7]. For these algorithms, the building blocks are quantities in which at least one external leg is off shell (in contrast to the on-shell recursion relations [8,9] described later in this article). These recursion relations were first constructed in the QCD context by Berends and Giele [6], and applied early on to matrix elements for backgrounds to top quark production [10].

For quite a while, simpler processes have been incorporated into parton-shower Monte Carlo programs that provide realistic event simulation at the hadron level. These programs, including PYTHIA [11] and HERWIG [12], perform parton showering and hadronization. They implement an approximation to the perturbative expansion that resums leading logarithms. More complex processes are now being included in this framework, using leading-order parton-level matrix elements provided by MADGRAPH or ALPGEN, for example, combined with a matching scheme [13] that avoids double-counting between the leading-order matrix elements and the parton shower. Yet these leading-order results often have a strong sensitivity to higher-order corrections. Gluon-initiated processes are particularly sensitive. For example, the cross section for production of the Standard Model Higgs boson via gluon-fusion at the LHC is boosted by roughly a factor of two as one goes from leading order to next-to-next-to-leading order (NNLO) in the perturbative QCD expansion [14].

For this reason, quantitative estimates for most processes require a calculation at next-to-leading order (NLO). Ideally, one would also match such results to a parton-shower Monte Carlo as well [15,16]. For a growing list of processes, this has been achieved, particularly within the program MC@NLO [15].

NLO calculations require knowledge of both virtual and real-emission corrections to the basic process. The real-emission corrections are constructed from tree-level amplitudes with one additional parton present, either an additional gluon, or a quark–antiquark pair replacing a gluon in the LO process. They can be computed using the same tree-level techniques used for the basic process. In addition, we need a method for extracting the infrared singularities arising from integration of the real-emission contributions over unresolved regions of phase space. These singularities cancel against those in the virtual

corrections or against counterterms from the evolution of parton distributions. Several such methods have been developed for use in generic NLO processes [17,18,19,20]. Subtraction methods based on dipole subtraction [19,20] are the most widely used today. A related subtraction method, based on so-called antenna factorization [21], has even been extended to NNLO [22]. In this review, we will focus on techniques for computing the virtual one-loop corrections to processes. Once the virtual corrections are known, their incorporation into a numerical program for the full NLO result is straightforward, because they do not need to be integrated over unresolved regions of phase space, and all of their infrared singularities will be manifest.

The computation of one-loop virtual corrections for processes with multiple partons, plus electroweak particles, is the bottleneck currently limiting availability of NLO results. The state of the art for complete computations is processes with up to three objects — jets, vector bosons, or scalars — in the final state (see *e.g.* refs. [23,24,25,26,27,28,29]). A number of new approaches aimed at one-loop multi-parton amplitudes are currently under development. Some are already producing results applicable to processes with four final-state objects. These approaches fall into three basic categories: improved traditional (including semi-numerical) [30,31,32,33,34,35,36,37,38,39,40,41,42], purely numerical [43,29], and on-shell analytic [44,45,46,47,48,49,50,51,52,53,54,55,56,57,58,59,60].

The semi-numerical approach of Ellis, Giele and Zanderighi [38] has already been used to compute loop corrections to the amplitudes involving a Higgs boson and four external partons [36], and to the six-gluon amplitude [39]. Nagy and Soper [43] have proposed a subtraction method for use in a purely numerical evaluation of one-loop amplitudes, and have evaluated the six-photon helicity amplitudes purely numerically [61]. The six-photon result has been reproduced very recently using both on-shell analytical and semi-numerical methods [62,63]. Binoth *et al.* [37] have developed a combined algebraic/numerical algorithm for multi-parton amplitudes; the algebraic part has been used to determine the rational parts of several types of amplitudes, including the six-photon amplitude (for which the rational parts vanish). The full algorithm is also being incorporated into a NLO QCD framework by the GRACE collaboration [32]. A purely numerical approach combining sector decomposition and contour deformations has recently been used to calculate tri-vector boson production [29]. Denner and Dittmaier have developed a numerically stable method for reducing one-loop tensor integrals [33], which has been used in various electroweak processes, but also in NLO QCD computations, including the production of a top quark pair in association with a jet at hadron colliders [28].

In this review we describe on-shell analytic methods for one-loop computations. The ‘on-shell’ terminology means that essentially all information is extracted from simpler (lower-loop and lower-point) amplitudes for physical states. In contrast, the conventional Feynman-diagram approach requires building blocks with off-shell states. The on-shell approach effectively restricts the states used in a calculation to physical ones. The restriction falls on some internal as well as external states. The approach relies on three general properties of perturbative amplitudes in any field theory: factorization, unitarity, and the existence of a representation in terms of Feynman integrals. An earlier form of on-shell methods was used to compute the one-loop amplitudes for $e^+e^- \rightarrow Z \rightarrow 4$ partons and (by crossing) $pp \rightarrow W, Z + 2$ jets [64]. The latter have been implemented in the MCFM program [25]. More recently, all six-gluon helicity amplitudes have been computed (primarily) with these methods [44,45,48,50,51,57,55,56,40].

On-shell methods provide a means for determining scattering amplitudes directly from

their poles and cuts. Perturbative unitarity, applied to a one-loop amplitude, determines its branch cuts in terms of products of tree amplitudes [65]. The unitarity method [44,45] provides a technique for producing functions with the correct branch cuts in all channels. Its power is enhanced by relying on the decomposition of loop amplitudes into a basis of loop-integral functions. Matching the cuts with the cuts of basis integrals in this decomposition provides a direct and efficient means for producing expressions for amplitudes. It is most convenient to use dimensional regularization to handle both infrared and ultraviolet divergences in massless gauge-theory scattering amplitudes. We take the number of space-time dimensions to be $D = 4 - 2\epsilon$. We can use fully D -dimensional states and momenta in the unitarity method to obtain complete amplitudes, at least when all internal particles are massless [46]. (In the older language of dispersion relations [65], amplitudes can be reconstructed fully from cuts in D dimensions because of the convergence of dispersion integrals in dimensional regularization [66].) In most cases, however, it is much simpler to use four-dimensional states and momenta in the cuts. This procedure correctly yields all terms in the amplitudes with logarithms and polylogarithms [45], but it generically drops rational terms, which have to be recovered via another method.

The basic framework of the unitarity method was set up in refs. [44,45]. In ref. [64], generalized unitarity was introduced as a means for simplifying cut calculations, by limiting the number of integral functions contributing to a cut. These techniques were applied to a variety of calculations in QCD and supersymmetric gauge theories [67,68]. More recent improvements to the unitarity method, by Britto, Cachazo and Feng [49], use complex momenta within generalized unitarity, allowing for a simple and purely algebraic determination of all box integral coefficients. Britto, Buchbinder, Cachazo and Feng [51] have shown how triangle and bubble integral coefficients may be evaluated by extracting residues in contour integrals. This approach has been used to compute various contributions to the six-gluon amplitude [51,57]. Very recently, Forde has proposed an efficient new approach to computing these coefficients [69].

The four-dimensional version of the unitarity method leaves undetermined additive rational-function terms in the amplitudes. These rational functions can be characterized by their kinematic poles. An efficient, systematic means for constructing these terms from their poles and residues is to use on-shell recursion relations [52,53,54,55,56], which were first devised by Britto, Cachazo, Feng and Witten, as a means for constructing tree-level amplitudes [8,9]. In a related development, Brandhuber *et al.* [70] and Anastasiou *et al.* [58] have investigated how to determine the rational parts of amplitudes from D -dimensional unitarity, extending earlier work [46,71]. Another approach to computing rational terms uses a clever organization of Feynman diagrams, together with the observation that only a limited set of tensor integrals can contribute to the rational terms [40,41]. Brandhuber *et al.* [72] have argued that rational terms can be obtained using a set of Lorentz-violating counterterms. Finally, Ossola, Papadopoulos and Pittau [42,63] have developed a new loop-integral decomposition method, which we expect will mesh well with generalized unitarity techniques reviewed here.

Most of the recent development of on-shell techniques at one loop has focused on QCD amplitudes in which all of the external particles are gluons. Amplitudes containing massless external quarks pose no inherent difficulty. The same basis of integrals can be used, and individual amplitudes should have comparable analytic complexity. However, they have fewer discrete symmetries, so the number of amplitudes that need to be computed is larger for the same total number of partons. Amplitudes with external electroweak

particles (vector bosons or Higgs bosons) in addition to QCD partons are of even greater phenomenological interest. Such amplitudes can also be built from the same basis of integrals. (For amplitudes with massive internal lines, such as in top-quark production, additional integrals are required.) In this review, in order to simplify the discussion, we focus primarily on amplitudes with external gluons only.

Recent years have also seen the emergence of on-shell methods at tree level, which have provided a basis for some of the recent developments at one loop. We will give some tree-level examples, but refer the reader to refs. [73,74,75] for a more extensive exposition.

It is also worth noting that the improved understanding of the structure of scattering amplitudes, stemming from on-shell methods, has also led to advances in more theoretical issues related to the AdS/CFT conjecture and in quantum gravity – see *e.g.* refs. [76].

This review is organized as follows. In section 2 we describe how the use of complex momenta is intrinsic to on-shell methods. In section 3 we review the BCFW on-shell recursion relations for tree amplitudes, giving a few examples. We turn to one-loop amplitudes in section 4, where we describe the unitarity-based method and some recent improvements. In section 5, we show how on-shell recursion is an efficient way to construct rational terms in one-loop amplitudes. We give our conclusions in section 6, and comment on the prospects for evaluating new amplitudes of phenomenological interest at the LHC with these methods.

2. Uses of Complex Kinematics

Multi-parton amplitudes in QCD are functions of a large number of variables, describing polarization states, color quantum numbers, and kinematics. It is important to disentangle the dependence on all these variables to as great an extent as possible. In this section we focus on techniques for separating and simplifying the kinematic behavior. The polarization-state dependence may be handled efficiently by computing helicity amplitudes, using the spinor-helicity formalism for external gluons [77,78].

The color dependence can be organized using the notion of color-ordered subamplitudes, or primitive amplitudes. Primitive amplitudes are defined for specific cyclic orderings of the external partons, but carry no explicit color indices. They can be computed using ‘color-ordered’ Feynman diagrams. Such diagrams can be drawn on the plane for the specified external ordering of the partons. (There are also restrictions on the direction of fermion flow through the diagrams in loop amplitudes.) The color indices have been stripped from all the vertices and propagators for these diagrams. The full amplitude can be assembled from the primitive amplitudes by dressing them with appropriate color factors.

For example, for n -gluon amplitudes, the tree-level color factors have the form of single traces, $\text{tr}(T^{a_1} T^{a_2} \dots T^{a_n})$, where T^{a_i} is an $SU(N_c)$ generator matrix in the fundamental representation, for gluon i [79,78]. The coefficients of these color structures define the tree-level primitive amplitudes $A_n^{\text{tree}}(1, 2, 3, \dots, n)$. At one loop, the n -gluon color factors can be either single traces — with an additional factor of N_c present — or double traces. The coefficients of the single traces, which would dominate in the large- N_c limit, are given directly by one-loop primitive amplitudes. The coefficients of the double traces are given by sums over permutations of primitive amplitudes [80,44,71]. Therefore we can focus on the coefficients of $N_c \text{tr}(T^{a_1} T^{a_2} \dots T^{a_n})$, which we denote here by $A_n^{1\text{-loop}}(1, 2, 3, \dots, n)$.

(Elsewhere in the literature, they are often denoted $A_{n;1}$, to distinguish them from the double-trace coefficients $A_{n;c}$ for $c > 1$.) The one-loop primitive amplitudes $A_n^{1\text{-loop}}$ have the same symmetry under cyclic permutations of the external legs as the tree amplitudes A_n^{tree} . Similar results hold when external quarks — fermions in the fundamental representation — are present as well [81]. We refer the reader to previous reviews [78,71] for a more complete description of helicity and color decompositions.

In this review, we concentrate on methods for computing the building blocks, primitive helicity amplitudes, which are functions only of the kinematic variables. A key property of primitive amplitudes is that their singularities, branch cuts (at loop level) as well as factorization poles, depend only on a restricted set of kinematic variables. This set consists of the squares of sums of cyclically adjacent momenta, $K_{i\dots j} = k_i + k_{i+1} + \dots + k_{j-1} + k_j$, where all indices are taken modulo n . Furthermore, the singularities are determined by lower-loop primitive amplitudes in the case of cuts, and by lower-point primitive amplitudes in the case of poles. This reducibility suggests the possibility of developing a recursive computational framework.

The singularity information can be accessed more easily if we define primitive amplitudes for suitable complex, yet on-shell, values of the external momenta. This simple observation came out of Witten’s development of twistor string theory [82], and many subsequent papers sparked by that article. Witten’s work demonstrated a remarkable simplicity for tree amplitudes, and suitable parts of loop amplitudes, when they were mapped into the twistor space of Penrose [83] in which twistor strings propagate. This space can be defined as a ‘half Fourier transform’ of the space of left- and right-handed two-component (Weyl) spinors $u_{\pm}(k_i)$ associated with a massless vector, $k_i^2 = 0$. The left-handed spinors are Fourier transformed, while the right-handed spinors remain as coordinates.

Here we will not rely directly on any concrete properties of twistor space. However, two conceptual ideas from that work underpin our approach:

- (i) Use two-component spinor variables as the independent variables for scattering processes, rather than four-component momenta.
- (ii) Treat opposite-helicity spinors as independent variables. For real Minkowski momenta, there is a complex-conjugation relation between the two. This treatment requires momenta to be generically complex.

Complex momenta are certainly not a new notion. Wick rotation allows the analytic properties of amplitudes for real Minkowski momenta to be deduced by continuation from the Euclidean region, in which the time components of Minkowski momenta are imaginary. Similarly, the complex analyticity of the S matrix, expressed as a function of the Lorentz-invariant products $s_{ij} = 2k_i \cdot k_j$, depends implicitly on having complex momenta k_i . On the other hand, arriving at complex momenta by thinking of the spinor variables as fundamental, leads to new ways of organizing the kinematic properties of helicity amplitudes.

2.1. Complex Kinematics and the Three-point Amplitude

The first hint that this approach might be useful comes from investigating three-point helicity amplitudes [82], displayed in fig. 1(a). For real momenta, an on-shell process with three external massless legs i, j, k is always singular, because $s_{ij} = 0$ for all three pairs of

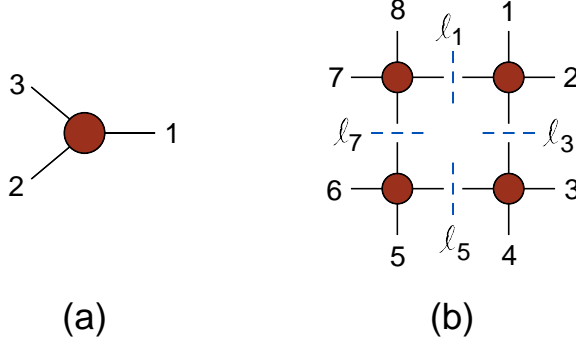


Fig. 1. Two types of processes involving massless particles for which complex momenta are very useful: (a) three-point amplitudes, and (b) generalized unitarity cuts.

legs. These conditions force the three momenta to be collinear with each other — if they are real — which in turn makes all kinematic quantities vanish. Using complex momenta to define the amplitude for three massless particles is also not a new idea. For example, Goroff and Sagnotti [84] used complex momenta to define non-singular three-graviton kinematics, in their on-shell computation of the two-loop divergence in pure Einstein gravity. However, there is a natural way to take the kinematics to be complex using spinor variables, which meshes neatly with the structure of helicity amplitudes.

First we introduce a shorthand notation for the two-component (Weyl) spinors associated with an n -parton process [82]:

$$(\lambda_i)_\alpha \equiv [u_+(k_i)]_\alpha, \quad (\tilde{\lambda}_i)_{\dot{\alpha}} \equiv [u_-(k_i)]_{\dot{\alpha}}, \quad i = 1, 2, \dots, n. \quad (2.1)$$

It is also convenient to describe the spinors with a ‘bra’ and ‘ket’ notation,

$$\lambda_i = |i^+\rangle = \langle i^-|, \quad \tilde{\lambda}_i = |i^-\rangle = \langle i^+|. \quad (2.2)$$

One can always reconstruct the momenta from the spinors, using the positive-energy projector for massless spinors, $u(k)\bar{u}(k) = \not{k}$, or

$$k_i^\mu (\sigma_\mu)_{\alpha\dot{\alpha}} = (\not{k}_i)_{\alpha\dot{\alpha}} = (\lambda_i)_\alpha (\tilde{\lambda}_i)_{\dot{\alpha}}. \quad (2.3)$$

Equation (2.3) shows that a massless momentum vector, written as a bi-spinor, is simply the product of a left-handed spinor with a right-handed one. This result is also valid for complex momenta.

Lorentz-invariant spinor products can be defined using the antisymmetric tensors $\varepsilon^{\alpha\beta}$ and $\varepsilon^{\dot{\alpha}\dot{\beta}}$ for the $SU(2)$ factors in the Lorentz algebra, $SL(2, R) \sim SU(2)_L \times SU(2)_R$:

$$\langle j l \rangle = \varepsilon^{\alpha\beta} (\lambda_j)_\alpha (\lambda_l)_\beta = \bar{u}_-(k_j) u_+(k_l), \quad (2.4)$$

$$[j l] = \varepsilon^{\dot{\alpha}\dot{\beta}} (\tilde{\lambda}_j)_{\dot{\alpha}} (\tilde{\lambda}_l)_{\dot{\beta}} = \bar{u}_+(k_j) u_-(k_l). \quad (2.5)$$

(The sign of $[j l]$ in eq. (2.5) matches that in most of the QCD literature; in much of the ‘twistor’ literature, *e.g.* refs. [82, 49, 8, 9], the opposite sign is used.) These products are antisymmetric, $\langle j l \rangle = -\langle l j \rangle$, $[j l] = -[l j]$. The usual momentum dot products can be constructed from the spinor products using the relation,

$$\langle l j \rangle [j l] = \frac{1}{2} \text{Tr}[\not{k}_j \not{k}_l] = 2k_j \cdot k_l = s_{jl}. \quad (2.6)$$

We will also use the notation

$$\langle a^- | K_{r\dots s} | b^- \rangle = \bar{u}_-(k_a) \gamma_\mu u_-(k_b) K_{r\dots s}^\mu = \sum_{i=r}^s \langle a i \rangle [i b] , \quad (2.7)$$

$$\langle a^- | K_{r\dots s} c | b^+ \rangle = \sum_{i=r}^s \langle a i \rangle [i c] \langle c b \rangle , \quad (2.8)$$

where the sums run over cyclically ordered labels between r and s , as well as,

$$s_{r\dots s} = K_{r\dots s}^2 , \quad s_{jlm} = (k_j + k_l + k_m)^2 . \quad (2.9)$$

Parity acts on a helicity amplitude by flipping the sign of all helicities. This symmetry may be implemented by exchanging the left- and right-handed spinor products in the amplitude, $\langle j l \rangle \leftrightarrow [l j]$.

For real momenta, λ_i and $\tilde{\lambda}_i$ are complex conjugates of each other. Therefore the spinor products are complex square roots of the Lorentz products,

$$\langle j l \rangle = \sqrt{s_{jl}} e^{i\phi_{jl}} , \quad [j l] = \pm \sqrt{s_{jl}} e^{-i\phi_{jl}} . \quad (2.10)$$

In this case, if all the s_{jl} vanish, then so do all the spinor products. However, for complex momenta, eq. (2.10) does not hold. In fact, it is possible to choose all three left-handed spinors to be proportional, $\tilde{\lambda}_1 = c_1 \tilde{\lambda}_3$, $\tilde{\lambda}_2 = c_2 \tilde{\lambda}_3$, while the right-handed spinors are not proportional, but obey the relation, $c_1 \lambda_1 + c_2 \lambda_2 + \lambda_3 = 0$, which follows from momentum conservation, $k_1 + k_2 + k_3 = 0$, and eq. (2.3). Then

$$[1 2] = [2 3] = [3 1] = 0 , \quad (2.11)$$

while $\langle 1 2 \rangle$, $\langle 2 3 \rangle$ and $\langle 3 1 \rangle$ are all nonvanishing.

For this kinematical choice, the tree-level primitive amplitude for two negative helicities and one positive helicity, A_3^{tree} , is nonsingular, even though all momentum invariants s_{jl} vanish according to eq. (2.6). (We assign helicities to particles under the assumption that they are outgoing; if a particle is incoming, its true helicity is opposite to the label.) For three gluons, A_3^{tree} can be evaluated using the three-gluon-vertex in the color-ordered Feynman rules [71], as

$$A_3^{\text{tree}}(1^-, 2^-, 3^+) = \frac{i}{\sqrt{2}} \left[\varepsilon_1^- \cdot \varepsilon_2^- \varepsilon_3^+ \cdot (k_1 - k_2) + \varepsilon_2^- \cdot \varepsilon_3^+ \varepsilon_1^- \cdot (k_2 - k_3) + \varepsilon_3^+ \cdot \varepsilon_1^- \varepsilon_2^- \cdot (k_3 - k_1) \right] . \quad (2.12)$$

In the spinor-helicity formalism [77,78], the polarization vectors ε_i^\pm are expressed as,

$$\varepsilon_i^{\pm, \mu} = \varepsilon^{\pm, \mu}(k_i, q_i) = \pm \frac{\langle q_i^\mp | \gamma^\mu | k_i^\mp \rangle}{\sqrt{2} \langle q_i^\mp | k_i^\pm \rangle} , \quad (2.13)$$

in terms of null reference momenta q_i , which may be chosen to simplify the computation. In eq. (2.12), if we choose $q_2 = q_1$ and $q_3 = k_1$, then $\varepsilon_1^- \cdot \varepsilon_2^- = \varepsilon_3^+ \cdot \varepsilon_1^- = 0$. Upon using a Fierz rearrangement and momentum conservation, the lone surviving term in eq. (2.12) becomes,

$$\begin{aligned}
A_3^{\text{tree}}(1^-, 2^-, 3^+) &= i\sqrt{2} \, \varepsilon_2^- \cdot \varepsilon_3^+ \, \varepsilon_1^- \cdot k_2 \\
&= i \frac{[q_1 3] \langle 1 2 \rangle}{[q_1 2] \langle 1 3 \rangle} \frac{[q_1 2] \langle 2 1 \rangle}{[q_1 1]} \\
&= i \frac{\langle 1 2 \rangle^2}{\langle 3 1 \rangle} \frac{[q_1 3]}{[q_1 1]} \frac{\langle 3 2 \rangle}{\langle 3 2 \rangle} \\
&= -i \frac{\langle 1 2 \rangle^2}{\langle 3 1 \rangle} \frac{[q_1 1] \langle 1 2 \rangle}{[q_1 1] \langle 3 2 \rangle}, \tag{2.14}
\end{aligned}$$

or

$$A_3^{\text{tree}}(1^-, 2^-, 3^+) = i \frac{\langle 1 2 \rangle^4}{\langle 1 2 \rangle \langle 2 3 \rangle \langle 3 1 \rangle}. \tag{2.15}$$

Equation (2.15) is the first member of the sequence of Parke-Taylor, or maximally-helicity-violating (MHV), tree amplitudes for n gluons [85,86,87],

$$A_n^{\text{tree MHV}, jk} \equiv A_n^{\text{tree}}(1^+, \dots, j^-, \dots, k^-, \dots, n^+) = i \frac{\langle j k \rangle^4}{\langle 1 2 \rangle \langle 2 3 \rangle \dots \langle n 1 \rangle}. \tag{2.16}$$

In this expression, only gluons j and k have negative helicity; the remaining $(n-2)$ gluons have positive helicity. For $n \geq 4$, these amplitudes are well-defined for real momenta. However, for $n = 3$, formula (2.15) only makes sense for complex momenta of the type (2.11).

There is a class of complex momenta conjugate to eq. (2.11), for which

$$\langle 1 2 \rangle = \langle 2 3 \rangle = \langle 3 1 \rangle = 0, \tag{2.17}$$

while $[1 2]$, $[2 3]$ and $[3 1]$ are all nonvanishing. Such momenta make the parity-conjugate three-point amplitude,

$$A_3^{\text{tree}}(1^+, 2^+, 3^-) = -i \frac{[1 2]^4}{[1 2] [2 3] [3 1]}, \tag{2.18}$$

well-defined. When the amplitude $A_3^{\text{tree}}(1^-, 2^-, 3^+)$ appears in the ‘wrong’ kinematics (2.17), it should be set to zero, because more vanishing spinor products appear in the numerator than in the denominator.

For any on-shell complex momenta, the all-positive amplitude vanishes,

$$A_3^{\text{tree}}(1^+, 2^+, 3^+) = 0. \tag{2.19}$$

This result follows easily by choosing all reference momenta q_i to be the same, which forces $\varepsilon_i^+ \cdot \varepsilon_j^+$ to vanish for all pairs i, j . The same result holds for $A_3^{\text{tree}}(1^-, 2^-, 3^-)$, of course. In a similar fashion, the three-point amplitude for a pair of massless quarks (which must carry opposite helicity) plus one gluon is well-defined and nonzero using the kinematics (2.11) if the gluon helicity is negative, and using the kinematics (2.17) if it is positive. It vanishes for the ‘wrong’ kinematics. These rules will become important later for evaluating generalized unitarity cuts and recursive diagrams containing three-point vertices.

2.2. Complex Kinematics to Utilize Factorization Information

We have seen how suitable complex kinematics can simplify the structure of the three-point amplitude. Much more significantly, however, complex kinematics allow the exploration of generic factorization singularities of on-shell amplitudes, and the use of factorization information to reconstruct the amplitude, as was recognized at tree-level by Britto, Cachazo, Feng and Witten (BCFW) [9]. We will review the BCFW recursion relations in the next section. Here we shall just discuss the simple example of the Parke-Taylor amplitudes. The idea is to embed a tree amplitude A_n^{tree} into a one-complex-parameter family of on-shell amplitudes $A_n^{\text{tree}}(z)$. The rationale for introducing the complex parameter z is that it allows us to apply the full power of complex variable theory to reconstruct amplitudes from their poles. The simplest way to introduce this parameter is by modifying, or ‘shifting’ the momenta of just two of the n partons, in a way that keeps them on shell. Because of eq. (2.3), the two momenta will automatically remain on shell if we shift the spinor variables, and then define the shifted momenta to be the products of the new left- and right-handed spinors.

We define the $[j, l]$ shift to be [9],

$$\tilde{\lambda}_j \rightarrow \tilde{\lambda}_j - z\tilde{\lambda}_l, \quad \lambda_l \rightarrow \lambda_l + z\lambda_j, \quad (2.20)$$

where z is a complex parameter. The shift leaves untouched λ_j , $\tilde{\lambda}_l$, and the spinors for all the other particles in the process. Under the shift, the corresponding momenta shift as,

$$\begin{aligned} k_j^\mu &\rightarrow k_j^\mu(z) = k_j^\mu - \frac{z}{2} \langle j^- | \gamma^\mu | l^- \rangle, \\ k_l^\mu &\rightarrow k_l^\mu(z) = k_l^\mu + \frac{z}{2} \langle j^- | \gamma^\mu | l^- \rangle, \end{aligned} \quad (2.21)$$

which preserves their masslessness, $k_j^2(z) = 0 = k_l^2(z)$, as well as overall momentum conservation.

Suppose we apply the $[n, 1]$ shift, $\tilde{\lambda}_n \rightarrow \tilde{\lambda}_n - z\tilde{\lambda}_1$, $\lambda_1 \rightarrow \lambda_1 + z\lambda_n$, to the MHV amplitude (2.16), for the case $k = n$ (and $j \neq 1$). Because the formula contains only right-handed λ_i spinors, the only induced z dependence arises from terms containing λ_1 . The spinor product $\langle 1 2 \rangle$ is shifted to $\langle 1 2 \rangle \rightarrow \langle 1 2 \rangle + z \langle n 2 \rangle$. The spinor product $\langle n 1 \rangle$ is unaffected, because $\langle n 1 \rangle \rightarrow \langle n 1 \rangle + z \langle n n \rangle$, but $\langle n n \rangle = 0$ by antisymmetry. Thus the MHV amplitude becomes

$$A_n^{\text{tree MHV}, jn}(z) = i \frac{\langle j n \rangle^4}{(\langle 1 2 \rangle + z \langle n 2 \rangle) \langle 2 3 \rangle \cdots \langle n 1 \rangle}. \quad (2.22)$$

If we divide this shifted amplitude by z , we get a function with two poles at finite z , one at the origin and one at $z = -\langle 1 2 \rangle / \langle n 2 \rangle$, as shown in fig. 2. The function behaves like $1/z^2$ as $z \rightarrow \infty$, so the integral around the circle C at infinity vanishes,

$$0 = \oint_C \frac{dz}{2\pi i} \frac{A_n^{\text{tree MHV}, jn}(z)}{z}. \quad (2.23)$$

Cauchy’s theorem then guarantees that the two poles at finite z have equal and opposite residue.

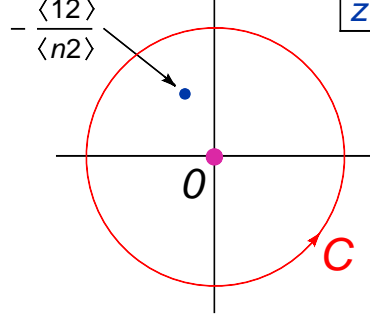


Fig. 2. Analytic structure of $A_n^{\text{tree MHV}, j^n}(z)/z$ under the $[n, 1]$ shift.

The residue of the pole at the origin is simply the MHV amplitude we want to compute, $A_n^{\text{tree MHV}, j^n}(0) = A_n^{\text{tree MHV}, j^n} \equiv A_n$. The residue of the second pole is determined by the factorization properties of the amplitude, because it occurs at the point that the intermediate momentum $K_{12}(z) \equiv k_1(z) + k_2$ goes on shell, $K_{12}^2(z) = (\langle 12 \rangle + z \langle n2 \rangle) [21] \rightarrow 0$. That is, at the value $z = z_{12} \equiv -\langle 12 \rangle / \langle n2 \rangle$ we have,

$$\begin{aligned} \hat{\langle 12 \rangle} &= \langle 12 \rangle + z_{12} \langle n2 \rangle = 0, \\ [\hat{1}2] &= [12] \neq 0, \\ s_{\hat{1}2} &= \langle \hat{1}2 \rangle [2\hat{1}] = 0. \end{aligned} \tag{2.24}$$

A hat on a kinematic variable means that a shift of the form (2.20) has been applied to the variable, with z then fixed to the value that puts an intermediate momentum on shell. The key point is that, because an intermediate state goes on shell, the amplitude factorizes at this point into the product of two lower-point amplitudes, multiplied by the diverging propagator. In general there is a sum over the helicity h of the intermediate state, $h = \pm 1$ for intermediate gluons.

Equating the residue at $z = z_{12}$ to the negative of the one at the origin, we have

$$\begin{aligned} A_n^{\text{tree}} &= \sum_{h=\pm} A_{n-1}^{\text{tree}}(\hat{K}_{12}^h, 3^+, \dots, j^-, \dots, \hat{n}^-) \\ &\quad \times \left[-\text{Res}_{z=z_{12}} \left(\frac{1}{z} \frac{i}{\hat{K}_{12}^2(z)} \right) \right] A_3^{\text{tree}}(\hat{1}^+, 2^+, -\hat{K}_{12}^{-h}) \\ &= A_{n-1}^{\text{tree}}(\hat{K}_{12}^+, 3^+, \dots, j^-, \dots, \hat{n}^-) \frac{i}{s_{12}} A_3^{\text{tree}}(\hat{1}^+, 2^+, -\hat{K}_{12}^-). \end{aligned} \tag{2.25}$$

In the second step we evaluated the residue in brackets, and used the vanishing of $A_3^{\text{tree}}(1^+, 2^+, 3^+)$ in eq. (2.19) to reduce the helicity sum to a single term.

Equation (2.25) is the prototype for the tree-level BCFW recursion relation reviewed in section 3. In general, there will be several terms on the right-hand side, corresponding to different nontrivial factorization channels which can be probed for suitable values of z . The MHV amplitudes are unique in having no multi-particle poles, which is related to the vanishing of n -gluon amplitudes with fewer negative helicities,

$$A_n^{\text{tree}}(1^\pm, 2^+, 3^+, \dots, n^+) = 0. \tag{2.26}$$

For this reason, the recursion relation (2.25) in the MHV case has but a single term.

We can further evaluate eq. (2.25) using the explicit form (2.16) of the MHV amplitudes, as a simple exercise in manipulating the hatted variables that appear, and as an on-shell recursive proof of the formula. (As an historical note, the first proof of eq. (2.16) employed recursion relations of the off-shell variety [6].) Inserting the forms of the $(n-1)$ -point and three-point amplitudes, eq. (2.25) becomes,

$$A_n^{\text{tree}} = \frac{i \langle j \hat{n} \rangle^4}{\langle \hat{K}_{12} 3 \rangle \langle 3 4 \rangle \cdots \langle (n-1) \hat{n} \rangle \langle \hat{n} \hat{K}_{12} \rangle} \frac{i}{s_{12}} \frac{-i [\hat{1} 2]^3}{[2 (-\hat{K}_{12})] [(-\hat{K}_{12}) \hat{1}]} . \quad (2.27)$$

We need to continue the spinors for $(-\hat{K}_{12})$ into those for \hat{K}_{12} . Because a pair of such spinors appears, we pick up a minus sign. (Determining the sign for the case of an intermediate quark line is more subtle.)

Because the $[n, 1]$ shift leaves $\tilde{\lambda}_1$ and λ_n alone, we can let $\hat{n} \rightarrow n$ and $\hat{1} \rightarrow 1$ in eq. (2.27). Because the shifted momentum is proportional to $\tilde{\lambda}_1 \lambda_n$, a hatted momentum appearing in a right-handed spinor product with n , or in a left-handed spinor product with 1 , can have its hat removed as well. For this reason, it is very convenient to use factors of $\langle n \hat{K}_{12} \rangle$ and $[\hat{K}_{12} 1]$ to clean up other spinor products containing \hat{K}_{12} , inserting them into the numerator and denominator of expressions as needed. In the present case, the necessary factors are already present. Equation (2.27) becomes,

$$\begin{aligned} A_n^{\text{tree}} &= i \frac{\langle j n \rangle^4 [1 2]^3}{\langle 3 4 \rangle \cdots \langle (n-1) n \rangle \langle n^- | \hat{K}_{12} | 2^- \rangle \langle 3^- | \hat{K}_{12} | 1^- \rangle \langle 1 2 \rangle [1 2]} \frac{1}{\langle 1 2 \rangle [1 2]} \\ &= i \frac{\langle j n \rangle^4 [1 2]^3}{\langle 3 4 \rangle \cdots \langle (n-1) n \rangle \langle n 1 \rangle [1 2] \langle 3 2 \rangle [2 1] \langle 1 2 \rangle [1 2]} \frac{1}{\langle 1 2 \rangle [1 2]} \\ &= i \frac{\langle j n \rangle^4}{\langle 1 2 \rangle \langle 2 3 \rangle \langle 3 4 \rangle \cdots \langle (n-1) n \rangle \langle n 1 \rangle} . \end{aligned} \quad (2.28)$$

The final form indeed matches the expression (2.16), thus confirming it recursively.

2.3. Complex Kinematics for Generalized Unitarity

Figure 1(b) shows a second class of configurations for which complex kinematics are useful, namely generalized unitarity conditions, which will be discussed in more detail in section 4. At one loop, conventional unitarity constraints on amplitudes are analyzed by putting two intermediate states on shell. For example, if legs 1, 2, 3 and 4 in fig. 1(b) are outgoing, and legs 5, 6, 7 and 8 are incoming, then the conventional cut in the 1234 channel is computed by imposing $\ell_1^2 = \ell_5^2 = 0$. This constraint can be realized with all momenta real in Minkowski space. It can then be interpreted as a $4 \rightarrow 2$ particle scattering process, followed by a $2 \rightarrow 4$ particle scattering.

Generalized unitarity corresponds to requiring *more* than two internal particles to be on shell. Often these constraints cannot be realized with real Minkowski momenta. Suppose we try to add the condition $\ell_3^2 = 0$ to the standard cut constraints $\ell_1^2 = \ell_5^2 = 0$ in fig. 1(b). The problem is that $1 \rightarrow 3$ processes are forbidden for real, non-collinear massless momenta, although $2 \rightarrow 2$ processes are allowed. After setting $\ell_3^2 = 0$, fig. 1(b) contains a four-point subamplitude in which leg ℓ_1 is incoming, and legs 1 and 2 are

outgoing with s_{12} nonzero. We can arrange for this to be a real Minkowski process by taking ℓ_3 to be incoming. But then the subamplitude below it in the figure has only leg ℓ_5 incoming, and legs ℓ_3 , 3 and 4 outgoing. It cannot correspond to a real on-shell process, as long as s_{34} is nonzero.

Similarly, we cannot impose $\ell_7^2 = 0$ on top of $\ell_1^2 = \ell_5^2 = 0$, in the process $5 + 6 + 7 + 8 \rightarrow 1 + 2 + 3 + 4$, and still have real momenta. Typically then, one needs to allow for complex momenta in order to implement generalized cut conditions. As an even simpler example, if we consider a quadruple cut with fewer than the eight external momenta shown in fig. 1(b), then at least one tree amplitude will have only three external legs, and this fact alone dictates complex momenta.

On the other hand, generalized cut conditions *can* sometimes be satisfied with only real momenta. In fig. 1(b), suppose now that the scattering process has legs 4, 5, 6 and 7 incoming, and legs 8, 1, 2 and 3 outgoing. Then it is possible to solve all four internal constraints, $\ell_1^2 = \ell_3^2 = \ell_5^2 = \ell_7^2 = 0$, with real Minkowski momenta, corresponding to scattering that proceeds from the lower left to the upper right of the figure; that is, $5 + 6 \rightarrow \ell_7 + \ell_5$, followed by $\ell_7 + 7 \rightarrow 8 + \ell_1$ and $4 + \ell_5 \rightarrow \ell_3 + 3$, followed by $\ell_3 + \ell_1 \rightarrow 1 + 2$.

3. On-Shell Recursion for Tree Amplitudes

3.1. General Framework

In this section we describe the construction of tree amplitudes via on-shell recursion. As alluded to in the previous section, the BCFW recursion relation [8,9] is based on introducing a complex-parameter-dependent shift of two of the external massless spinors, as given in eq. (2.20). The construction of tree amplitudes via on-shell recursion essentially amounts to generalizing and reversing the steps in section 2.2. Instead of starting with a known amplitude, and verifying its analytic properties under the parameter-dependent shift, we use such properties to systematically construct unknown amplitudes.

Following the same procedure as for the MHV case in eq. (2.22), for generic amplitudes we define an analytically continued amplitude,

$$A(z) = A(k_1, \dots, k_j(z), k_{j+1}, \dots, k_l(z), \dots, k_n), \quad (3.1)$$

which remains on-shell, but depends on the complex parameter z . If A is a tree amplitude, then $A(z)$ is a rational function of z . The physical amplitude is given by $A(0)$.

Following the MHV case (2.23) consider the contour integral,

$$\frac{1}{2\pi i} \oint_C \frac{dz}{z} A(z), \quad (3.2)$$

where the contour is taken around the circle at infinity. If $A(z) \rightarrow 0$ as $z \rightarrow \infty$, the contour integral vanishes and we obtain a relationship between the physical amplitude, at $z = 0$, and a sum over residues for the poles of $A(z)$, located at z_α ,

$$A(0) = - \sum_{\text{poles } \alpha} \text{Res}_{z=z_\alpha} \frac{A(z)}{z}. \quad (3.3)$$

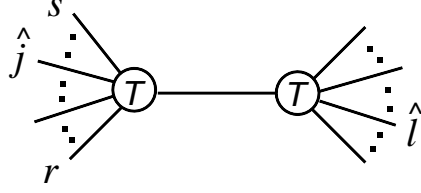


Fig. 3. Diagrammatic representation of one term in the tree-level recursion relation. The label ‘ T ’ refers to tree vertices, which are on-shell lower-point amplitudes. The momenta \hat{j} and \hat{l} undergo the $[j, l]$ shift in eq. (2.20). The two shifted legs must be attached to separate tree vertices.

To determine the residues at each pole, we use the general factorization properties that any amplitude must satisfy as an intermediate momentum K^μ goes on shell, $K^2 \rightarrow 0$. In general, the residue is given by a product of lower-point on-shell amplitudes. Only a subset of the possible factorization limits for an amplitude are explored by the z -dependent shift. Poles in the z plane can develop in any channel that has leg j on one side of the pole and leg l on the other side, because the intermediate momentum is z -dependent. Thus we can solve the on-shell condition,

$$\begin{aligned} 0 &= [K_{r\dots s}(z)]^2 = \left(k_r + k_{r+1} + \dots + k_j(z) + \dots + k_s\right)^2 \\ &= K_{r\dots s}^2 - z \langle j^- | K_{r\dots s} | l^- \rangle. \end{aligned} \quad (3.4)$$

The solution is

$$z_{rs} = \frac{K_{r\dots s}^2}{\langle j^- | K_{r\dots s} | l^- \rangle}. \quad (3.5)$$

A contribution to the recursion relation from this residue is illustrated diagrammatically in fig. 3. To get the precise form of the contribution, using eq. (3.3), we need to evaluate the residue (as we did in eq. (2.25) for a special case),

$$- \operatorname{Res}_{z=z_{rs}} \left(\frac{1}{z} \frac{i}{K_{r\dots s}^2(z)} \right) = \frac{i}{K_{r\dots s}^2}. \quad (3.6)$$

The final form of the tree-level recursion relation is [8,9]

$$A(0) = \sum_{r,s,h} A_L^h(z=z_{rs}) \frac{i}{K_{r\dots s}^2} A_R^{-h}(z=z_{rs}). \quad (3.7)$$

Generically we have a double sum, labeled by r, s , over recursive diagrams, with legs j and l always appearing on opposite sides of the pole. There is also a sum over the helicity h of the intermediate state. The squared momentum associated with the pole, $K_{r\dots s}^2$, arising from eq. (3.6), is evaluated in the unshifted kinematics. The on-shell tree amplitudes A_L and A_R are evaluated in kinematics that have been shifted by eq. (2.20), with $z = z_{rs}$. The shifted momenta for such kinematics are indicated by hats.

Equation (3.7) may alternatively be derived by expressing $A(z)$ as a sum over poles multiplied by their residues (under our assumption that $A(z) \rightarrow 0$ as $z \rightarrow \infty$). This representation, valid for all z , is

$$A(z) = \sum_{r,s,h} A_L^h(z = z_{rs}) \frac{i}{K_{r\dots s}^2 - z \langle j^- | K_{r\dots s} | l^- \rangle} A_R^{-h}(z = z_{rs}). \quad (3.8)$$

By setting $z = 0$ in this formula, we recover the recursion relation (3.7).

To derive the recursion relation, we assumed that the amplitude $A(z)$ vanishes as $z \rightarrow \infty$. If all the external particles are gluons, then the validity of this assumption depends only on the helicity of the two shifted legs. There are four different cases, which we can label by $[h_j, h_l] = [\pm, \pm]$. A shift of type $[+, -]$ does not generally make $A(z)$ vanish at infinity. As an example, the MHV amplitude (2.16) behaves as either z^2 or z^3 as $z \rightarrow \infty$, because of the factor of $\langle j k \rangle^4$ in the numerator. The case $[-, +]$ is the simplest to analyze because each individual Feynman diagram vanishes separately [9]. Shifts of type $[-, -]$ and $[+, +]$ also make the amplitude vanish as $z \rightarrow \infty$, but here cancellations between Feynman diagrams are required. The vanishing behavior has been proven using generalizations of the shift (2.20) that affect three or more momenta [88,75].

The on-shell recursion relation (3.7) contains spinor products involving hatted momenta. For the purposes of numerical evaluation, we can leave the amplitudes in this form, because the complex hatted momenta are built from well-defined spinors, whose inner products can be computed from eqs. (2.4) and (2.5). However, for analytic purposes it is useful to eliminate the hatted momenta in favor of external momenta. We can make use of the following relations,

$$\begin{aligned} \langle \hat{j} a \rangle &= \langle j a \rangle, & [\hat{j} a] &= [j a] - z_{rs} [l a], \\ [\hat{l} a] &= [l a], & \langle \hat{l} a \rangle &= \langle l a \rangle + z_{rs} \langle j a \rangle, \\ [\hat{K}_{r\dots s} a] &= \frac{\langle j^- | \hat{K}_{r\dots s} | a^- \rangle}{\langle j \hat{K}_{r\dots s} \rangle} = \frac{\langle j^- | K_{r\dots s} | a^- \rangle}{\langle j \hat{K}_{r\dots s} \rangle}, \\ \langle a \hat{K}_{r\dots s} \rangle &= \frac{\langle a^- | \hat{K}_{r\dots s} | l^- \rangle}{[\hat{K}_{r\dots s} l]} = \frac{\langle a^- | K_{r\dots s} | l^- \rangle}{[\hat{K}_{r\dots s} l]}, \\ [\hat{K}_{r\dots s} \hat{j}] &= \frac{-K_{r\dots s}^2 + 2k_j \cdot K_{r\dots s}}{\langle j \hat{K}_{r\dots s} \rangle}, \\ \langle \hat{K}_{r\dots s} \hat{l} \rangle &= -\frac{K_{r\dots s}^2 + 2k_l \cdot K_{r\dots s}}{[\hat{K}_{r\dots s} l]}. \end{aligned} \quad (3.9)$$

To simplify the expressions we used, for example,

$$\langle j^- | \hat{K}_{r\dots s} | a^- \rangle = \langle j^- | K_{r\dots s} | a^- \rangle - \frac{z_{rs}}{2} \langle j^- | \gamma_\mu | a^- \rangle \langle j^- | \gamma^\mu | l^- \rangle, \quad (3.10)$$

where the last term vanishes by a Fierz identity. The product $A_L^h \times A_R^{-h}$ is homogeneous in the spinors carrying the intermediate momentum $\hat{K}_{r\dots s}$. Because of this, any remaining factors of $\langle j \hat{K}_{r\dots s} \rangle$ and $[\hat{K}_{r\dots s} l]$ can be paired up to give factors of

$$\langle j \hat{K}_{r\dots s} \rangle [\hat{K}_{r\dots s} l] = \langle j^- | K_{r\dots s} | l^- \rangle. \quad (3.11)$$

Recursive diagrams containing three-point amplitudes often vanish because the ‘wrong’ kinematics are present. In general, if a $[j, l]$ shift is used, and the recursive diagram contains a three-vertex with two positive helicities, one of which is j , then the diagram vanishes. The reason is that the spinor λ_j is unaffected by the shift, so its product

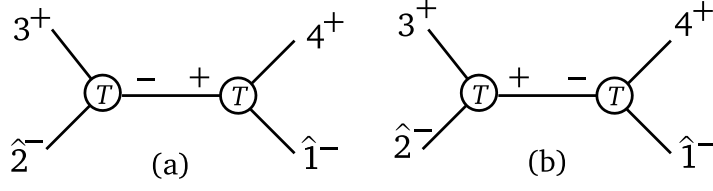


Fig. 4. The two on-shell recursive diagrams obtained from the $[1, 2]$ shift. The label ‘ T ’ in the blobs indicates that the vertices are tree amplitudes. Diagram (a) vanishes, as explained in the text.

with the spinor for the other external leg a in the three-point amplitude, $\langle j a \rangle$, remains nonvanishing. Therefore $[j a]$, and all of the left-handed spinor products, must vanish, and so the three-vertex with two positive helicities vanishes, as discussed in section 2. Similarly, three-vertices with two negative helicities can also be dropped, when one of the three legs is l .

3.2. Tree-level examples

As a first example, consider the amplitude $A_4^{\text{tree}}(1^-, 2^-, 3^+, 4^+)$. This amplitude can be constructed recursively from the three-point amplitudes given in eqs. (2.15) and (2.18). As discussed above, for the $[1, 2]$ shift (a $[-, -]$ shift) the amplitude vanishes for large z . Using this shift, there are two potential terms in the recursion relation, corresponding to diagrams (a) and (b) in fig. 4.

$$A_4^{\text{tree}}(1^-, 2^-, 3^+, 4^+) = D_4^{(a)} + D_4^{(b)}. \quad (3.12)$$

The first of these diagrams,

$$D_4^{(a)} = A_3^{\text{tree}}(\hat{2}^-, 3^+, -\hat{K}_{23}^-) \frac{i}{s_{23}} A_3^{\text{tree}}(4^+, \hat{1}^-, \hat{K}_{23}^+), \quad (3.13)$$

vanishes because of the ‘wrong’ kinematics discussed above.

Now evaluate diagram (b), using eqs. (2.15) and (2.18), with an overall minus sign for the continuation $-\hat{K}_{23} \rightarrow \hat{K}_{23}$,

$$\begin{aligned} D_4^{(b)} &= A_3^{\text{tree}}(\hat{2}^-, 3^+, -\hat{K}_{23}^+) \frac{i}{s_{23}} A_3^{\text{tree}}(4^+, \hat{1}^-, \hat{K}_{23}^-) \\ &= -i \frac{[3 \hat{K}_{23}]^3}{[\hat{2} 3] [\hat{K}_{23} \hat{2}]} \frac{1}{s_{23}} \frac{\langle \hat{1} \hat{K}_{23} \rangle^3}{\langle 4 \hat{1} \rangle \langle \hat{K}_{23} 4 \rangle}. \end{aligned} \quad (3.14)$$

This form is already satisfactory for the purpose of evaluating the amplitude numerically. It is, however, a useful exercise to eliminate hatted momenta in favor of unhatted external momenta. Applying the substitutions (3.9) and simplifying the expression for diagram (b), we find

$$A_4^{\text{tree}}(1^-, 2^-, 3^+, 4^+) = i \frac{\langle 1 2 \rangle^4}{\langle 1 2 \rangle \langle 2 3 \rangle \langle 3 4 \rangle \langle 4 1 \rangle}, \quad (3.15)$$

in agreement with the MHV formula (2.16).

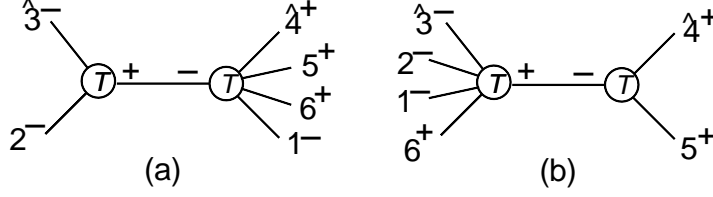


Fig. 5. The nonvanishing recursive diagrams for $A_6^{\text{tree}}(1^-, 2^-, 3^-, 4^+, 5^+, 6^+)$, using a $[3, 4]$ shift.

Interestingly, using the on-shell recursion relations, the four-point amplitude, and indeed all tree amplitudes, can be constructed from the on-shell three-vertices. The four-point vertex in the Yang-Mills Feynman rules is unnecessary. On the other hand, the four-point vertex is related by gauge invariance to the three-point vertex. Gauge invariance is necessary to decouple unphysical states. The recursion relations rely on the fact that such states are not present in factorization limits. In this way, they implicitly incorporate the correct four-point vertex.

Consider now the less trivial example of a six-point next-to-MHV (NMHV) amplitude, $A_6^{\text{tree}}(1^-, 2^-, 3^-, 4^+, 5^+, 6^+)$. Using a $[3, 4]$ shift (a $[-, +]$ shift) yields the two recursive diagrams in fig. 5,

$$A_6^{\text{tree}}(1^-, 2^-, 3^-, 4^+, 5^+, 6^+) = D_6^{(a)} + D_6^{(b)}. \quad (3.16)$$

The first of these diagrams gives,

$$D_6^{(a)} = A_3^{\text{tree}}(2^-, \hat{3}^-, -\hat{K}_{23}^+) \frac{i}{s_{23}} A_5^{\text{tree}}(\hat{4}^+, 5^+, 6^+, 1^-, \hat{K}_{23}^-) \quad (3.17)$$

$$= i \frac{\langle 2 \hat{3} \rangle^3}{\langle \hat{3} \hat{K}_{23} \rangle \langle \hat{K}_{23} 2 \rangle} \frac{1}{s_{23}} \frac{\langle 1 \hat{K}_{23} \rangle^3}{\langle \hat{4} 5 \rangle \langle 5 6 \rangle \langle 6 1 \rangle \langle \hat{K}_{23} \hat{4} \rangle}. \quad (3.18)$$

Applying eq. (3.9), we may rewrite this expression in terms of unhatted momenta, using the definitions in eqs. (2.7) and (2.9),

$$\begin{aligned} D_6^{(a)} &= i \frac{\langle 2 3 \rangle^3}{\langle 3^- | K_{23} | 4^- \rangle \langle 2^- | K_{23} | 4^- \rangle} \frac{1}{\langle 2 3 \rangle [3 2]} \\ &\quad \times \frac{\langle 1^- | K_{23} | 4^- \rangle^3}{(\langle 4 5 \rangle + [2 3] \langle 3 5 \rangle / [2 4]) \langle 5 6 \rangle \langle 6 1 \rangle s_{234}} \\ &= i \frac{\langle 2 3 \rangle^2}{\langle 3 2 \rangle [2 4] \langle 2 3 \rangle [3 4] [3 2]} \frac{1}{[3 2]} \\ &\quad \times \frac{[2 4] \langle 1^- | K_{23} | 4^- \rangle^3}{\langle 5^- | K_{34} | 2^- \rangle \langle 5 6 \rangle \langle 6 1 \rangle s_{234}} \\ &= i \frac{\langle 1^- | K_{23} | 4^- \rangle^3}{[2 3] [3 4] \langle 5 6 \rangle \langle 6 1 \rangle \langle 5^- | K_{34} | 2^- \rangle s_{234}}. \end{aligned} \quad (3.19)$$

Similarly, diagram (b) in fig. 5 is given by

$$D_6^{(b)} = A_5^{\text{tree}}(6^+, 1^-, 2^-, \hat{3}^-, \hat{K}_{45}^+) \frac{i}{s_{45}} A_3^{\text{tree}}(\hat{4}^+, 5^+, -\hat{K}_{45}^-)$$

$$= i \frac{\langle 3^- | K_{12} | 6^- \rangle^3}{[6\,1][1\,2]\langle 3\,4\rangle\langle 4\,5\rangle\langle 5^- | K_{61} | 2^- \rangle s_{345}}. \quad (3.20)$$

It is interesting that this kind of representation of the amplitude is intimately connected [89] to the forms in which tree amplitudes appear in the infrared singularities of certain one-loop amplitudes [68]. This feature is related to the appearance of denominator factors such as $\langle 5^- | K_{34} | 2^- \rangle$ at one loop, where they arise in the reduction of various loop integrals to a basic set of integrals. They can be thought of as spinor ‘square roots’ of certain Gram determinants.

The expression $\langle 5^- | K_{34} | 2^- \rangle$ vanishes on a subspace of phase space. For example, when K_{34}^μ is any linear combination of k_2^μ and k_5^μ , it vanishes using the massless Dirac equation, $\not{k}u_\pm(k) = 0$. Note that $\langle 5^- | K_{34} | 2^- \rangle = -\langle 5^- | K_{61} | 2^- \rangle$ by momentum conservation, and so the latter form also vanishes on the same subspace. This subspace does not correspond to physical factorizations of the amplitude, so $D_6^{(a)}$ and $D_6^{(b)}$ each have spurious singularities on it. However, their sum, the full amplitude A_6^{tree} , is nonsingular. In principle, a numerical program should check for small values of such spurious denominator factors, in order to avoid round-off errors. (Near a spurious singularity for the above representation (3.16), one could for example make use of a different shift (2.20), whose spurious singularities are located elsewhere.) On the other hand, the singularity is fairly mild, because only one power of $\langle 5^- | K_{34} | 2^- \rangle$ appears in the denominator.

Curiously, the introduction of denominators such as $\langle 5^- | K_{34} | 2^- \rangle$, gives a much more compact representation of amplitudes (for $n \geq 7$) than forms without such denominators. The compactness is basically due to the more manifest factorization properties of amplitudes constructed via on-shell recursion relations. For example, the representation (3.16) makes manifest the correct behavior $A_6^{\text{tree}} \sim 1/\sqrt{s_{i(i+1)}}$ as any pair of adjacent momenta become collinear, $k_i \parallel k_{i+1}$, because the spinor products are square roots of momentum invariants, as described in eq. (2.10).

3.3. Generalizations

Many applications of these techniques have already been carried out at tree level. In the case of n -gluon amplitudes, a closed-form formula for the ‘split helicity’ configuration, $A_n^{\text{tree}}(1^-, 2^-, \dots, i^-, (i+1)^+, \dots, n^+)$, has been constructed recursively, using essentially the same shift described above for $A_6^{\text{tree}}(1^-, 2^-, 3^-, 4^+, 5^+, 6^+)$ [90]. The recursion relations have been implemented numerically, and the computer time required for their evaluation is competitive with other methods [91].

In many circumstances it can be useful to generalize the shift to act on more than two spinor variables. For example, using the shift,

$$\tilde{\lambda}_1 \rightarrow \tilde{\lambda}_1 + z \langle 23 \rangle \tilde{\eta}, \quad \tilde{\lambda}_2 \rightarrow \tilde{\lambda}_2 + z \langle 31 \rangle \tilde{\eta}, \quad \tilde{\lambda}_3 \rightarrow \tilde{\lambda}_3 + z \langle 12 \rangle \tilde{\eta}, \quad (3.21)$$

for the case where gluons 1, 2 and 3 are of negative helicity and the rest are of positive helicity, and $\tilde{\eta}$ is an arbitrary left-handed spinor, the recursive diagrams that are generated [92] are in one-to-one correspondence with the MHV construction of Cachazo, Svrček and Witten [93,73]. The MHV construction was developed prior to the BCFW recursion relations. It provides a diagrammatic representation of tree amplitudes which

makes manifest their remarkable twistor-space properties [82,93]. It is quite interesting that these two different approaches can be directly connected.

Other types of shifts of multiple legs are useful because they can lead to improved behavior of the shifted amplitudes as $z \rightarrow \infty$. Such a shift was used to construct a recursion relation for the one-loop amplitudes $A_n^{1\text{-loop}}(1^+, 2^+, \dots, n^+)$ containing n identical-helicity gluons [52]. As mentioned above, multiple shifts can also be used to construct proofs of the proper large z behavior for tree amplitudes $A(z)$, under a standard shift of the form (2.20) [88,75].

The BCFW recursive analysis of n -gluon amplitudes was quickly extended to amplitudes with massless external quarks as well as gluons [94]. Recursion relations have also been established for tree-level amplitudes containing massive external particles, such as electroweak vector bosons, Higgs bosons, heavy quarks and squarks [88,95]. Processes in abelian theories such as QED can also be handled recursively [96]. The general recursive construction of all tree-level amplitudes in QCD with massive quarks has been described recently by Schwinn and Weinzierl [75]. In particular, they enumerate all possible standard shifts that lead to a vanishing amplitude $A(z)$ as $z \rightarrow \infty$.

4. The Unitarity-Based Method

Our goal is to compute a variety of one-loop amplitudes efficiently. For pedagogical reasons, we focus on higher-multiplicity multi-gluon amplitudes. Conventional Feynman-diagram methods in gauge theories involve unphysical states inside diagrams. This renders computations vastly more complicated than final results, because most of the computational effort is devoted to manipulating unphysical information which ultimately cancels out.

On-shell methods, as discussed in the Introduction, restrict states used in a calculation to physical states. For external gluons, the spinor-helicity basis imposes this restriction efficiently. We must also impose the restriction on internal states. We then rely on factorization, unitarity, and the existence of a representation in terms of Feynman integrals in order to compute amplitudes. We will also make use of several simplifications for the purely-massless amplitudes we are considering in this review.

4.1. Structure of the Amplitude

The first simplification comes from the use of color ordering, as mentioned in section 2. This reduces our problem to that of computing a color-ordered one-loop amplitude, in which external legs are ordered cyclicly. We can correspondingly introduce color-ordered Feynman diagrams, in which each vertex inherits an ordering from the overall ordering of the diagram. Although we do not want to use Feynman diagrams, not even the smaller set of color-ordered ones, to perform explicit computations, we can nonetheless imagine performing a gedanken calculation. By considering which Feynman diagrams would contribute to the amplitudes, and properties of the one-loop integrals they would generate, we shall arrive at a compact set of loop-integral functions, in terms of which we will ultimately express the amplitudes.

In a gauge theory, we have both trivalent and tetravalent vertices. Let us first consider the diagrams built only out of gluons. Any diagram with four-point vertices can be

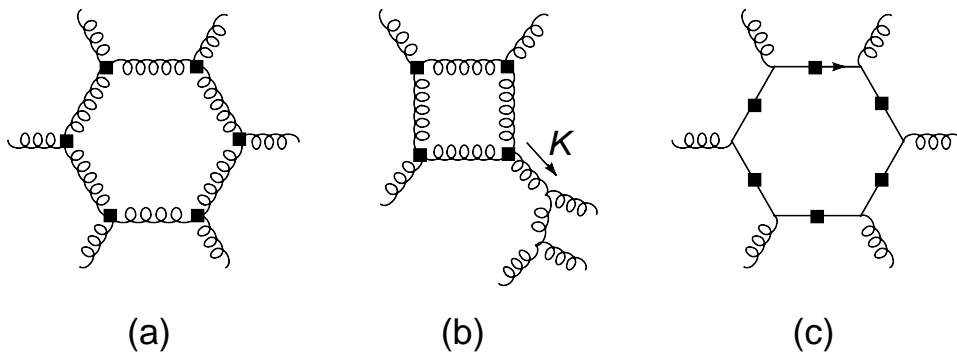


Fig. 6. (a) A ring diagram, for a gluon propagating in the loop. It contains the maximal possible powers of loop momenta in the numerator. Each black square, at a trivalent vertex, contributes one factor of loop momentum. (b) A non-ring diagram, in which some of the external legs attach to a tree which attaches to the loop. The momentum K is one of the momenta for the corresponding box integral. (c) A ring diagram for a quark in the loop; in this case the loop-momentum factors are associated with the fermion propagators.

obtained (possibly in more than one way) from a ‘parent’ diagram with all four-point vertices replaced by pairs of three-point vertices connected by a propagator. Diagrams with the maximal number of propagators inside the loop are thus ‘ring’ diagrams, built entirely out of three-point vertices; moreover, all external legs attach directly to vertices inside the loop, as shown in fig. 6(a). Accordingly, when computing an n -point amplitude, we must consider loop integrals with up to n external legs. We must also consider diagrams with fewer external legs attached directly to the loop, but rather attached to a tree which in turn attaches to the loop. These will give rise to loop integrals with fewer than n legs, but where some of the legs have momenta K which are sums of the original external momenta, as depicted in fig. 6(b). The original momenta may be massless (for gluons or massless quarks) or massive (for colorless heavy particles). The sums of momenta are in either case no longer massless; K^2 may be either positive or negative. That is, we must also consider loop integrals with external masses; but we may take all *internal* masses to be zero.

Each trivalent vertex contains terms proportional to the momenta flowing through it. If we consider the vertices within the loop, some of the terms contain a factor of the external momenta (or sums of external momenta). Others contain a factor of the loop momentum ℓ . The latter give rise to tensor integrals, in which tensors in the loop-momentum appear in the numerator. The maximal power of loop momentum arises when every vertex in the loop gives us one power, so that we get an n^{th} -rank n -point tensor integral. The (tensor) indices on the loop momenta are contracted into external momenta or polarization vectors. We will refer to integrals containing no powers of the loop momentum in the numerator as scalar integrals.

The above analysis holds equally well for gluons circulating in the loop as it does for scalar particles circulating there. (In fact, the contribution of a scalar particle in the adjoint representation of the gauge group accounts completely for the leading tensor-integral part of the gluon contribution.) For contributions of quarks in the loop, the counting starts out a bit differently. There are no powers of momenta at the vertices, of course, but the fermion propagator, $1/\ell = \ell/\ell^2$, supplies a factor ℓ proportional to the

loop momentum. As the number of vertices in the loop is the same as the number of propagators, fermionic contributions again give us integrals which range up to n^{th} -rank n -point tensor integrals, as illustrated in fig. 6(c).

We now wish to organize all of the loop integrals occurring in an amplitude, by reducing them down to some basic set. Tensor integrals can be reduced to scalar integrals, containing the same or fewer propagators, using traditional Brown–Feynman [97] or Passarino–Veltman [98] techniques, or using more recent spinorial techniques [99,100,101,42,35]. All these techniques effectively use Lorentz invariance to re-express integrals over powers of the loop momentum in terms of the metric and external momenta.

We will take all external vectors — both momenta and polarization vectors — to be strictly four dimensional. (For the polarization vectors, this is equivalent to adoption of the four-dimensional helicity scheme (FDH) [102,103].) For five- or higher-point integrals, any numerators can be expressed entirely in terms of differences of propagators and external Lorentz invariants. Each numerator factor has the form $\ell \cdot E$, where ℓ is the loop momentum and E is one of the external vectors. (A factor of ℓ^2 would cancel a propagator, immediately reducing the integral to a lower-point one.) With five or more external momenta k_i , satisfying momentum conservation, $\sum_i k_i = 0$, we can use four of them (massive or massless) as a basis to express any four-dimensional vector E . Then $\ell \cdot E$ becomes a linear combination of dot products $\ell \cdot k_j$, which in turn are differences of propagator denominators and invariants built from external momenta. After canceling propagators, we choose a new set of basis vectors for the daughter integrals, and repeat the process. Each step reduces the degree of the numerator by one, and may in addition reduce the number of external legs of the integrals by one.

For four- or lower-point integrals, we do not have enough independent external momenta to form a basis. We can instead use Lorentz invariance as above to re-express the integrals in terms of numerators involving the external momenta [97,98]. This reduction procedure again generates integrals with fewer numerator powers of the loop momentum, and possibly fewer external legs as well. At the end of this reduction, we are left only with scalar integrals having trivial numerators, with up to n external momenta.

Another option is to use not only external momenta in the basis, but also complex momenta built out of the associated spinors. The Lorentz products of the loop momentum with these complex momenta cannot cancel propagators; but a judicious choice will result in their integrals vanishing. Instead of expanding the external momenta in this basis, we could also choose to expand the four-dimensional components of the loop momentum. As we shall see in an example, this is particularly useful for evaluating one- and two-mass triangle and bubble integral contributions. In the case of a one-mass triangle with massless legs k_1 and k_2 , one can use the basis given by del Aguila and Pittau [35] (see also refs. [100,101]),

$$v_1^\mu = k_1^\mu, \quad v_2^\mu = k_2^\mu, \quad v_3^\mu = \langle 1^- | \gamma^\mu | 2^- \rangle, \quad \text{and } v_4^\mu = \langle 2^- | \gamma^\mu | 1^- \rangle. \quad (4.1)$$

For a two-mass triangle with massive legs K_1 and K_2 , and massless leg k_3 , a different basis is more appropriate,

$$v_1^\mu = K_1^\mu, \quad v_2^\mu = K_2^\mu, \quad v_3^\mu = \langle 3^+ | K_1 \gamma^\mu | 3^- \rangle, \quad \text{and } v_4^\mu = \langle 3^- | K_1 \gamma^\mu | 3^+ \rangle. \quad (4.2)$$

We can further reduce [104,99,105,106,33] all six- or higher-point scalar integrals to linear combinations of five- or lower-point integrals. This reduction is true to all orders

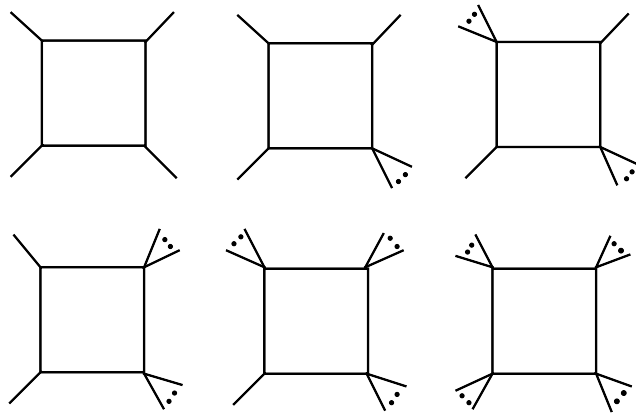


Fig. 7. The possible box integrals that can appear in one-loop amplitudes.

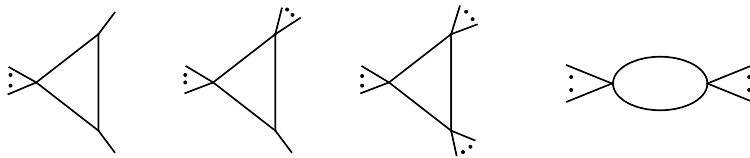


Fig. 8. The possible triangle and bubble integrals that can appear at one loop.

in the dimensional regulator $\epsilon = (4 - D)/2$. After the reduction, the five-point integrals that remain are all finite. They can be thought of as scalar pentagon integrals evaluated in six dimensions; such integrals are free of both ultraviolet and infrared divergences. They also appear multiplied by at least one explicit power of ϵ . If we were interested in computing amplitudes to $\mathcal{O}(\epsilon)$ or beyond, we would need to evaluate such pentagon integrals. If we are only interested in computing amplitudes to $\mathcal{O}(\epsilon^0)$, however, we may drop them.

Consequently, all amplitudes can ultimately be expressed in terms of ten different types of integrals: boxes with up to four external massive legs, triangles with up to three external massive legs, and bubbles. These integrals are shown in figs. 7 and 8. All internal propagators are massless, but each external momentum can be either massless or massive. Massive external momenta correspond to sums of the original massless or massive momenta of the amplitude. These integrals are all computed in dimensional regularization, which regulates both the ultraviolet divergences (which show up as single poles in bubble integrals) and the infrared divergences (which show up as double or single poles in the box and triangle functions).

Any color-ordered amplitude we wish to compute can therefore be expressed in terms of a standard basis of integrals,

$$A_n^{1\text{-loop}} = \sum_{j \in B} c_j \mathcal{I}_j. \quad (4.3)$$

For a given process, the integrals \mathcal{I}_j in the basis B are given *a priori* by the set of all functions defined in figs. 7 and 8, for all possible cyclicly-ordered combinations of momenta. These integrals have been tabulated, for example, in the first appendix in ref. [45]. The

coefficients c_j are rational functions of the external momenta and polarization vectors. Using the spinor-helicity basis, we express the c_j in terms of spinor products constructed from spinors corresponding to external momenta. The coefficients do in general depend on ϵ as well. Rational terms in amplitudes arise from ϵ terms striking ultraviolet poles in the integrals. (With the basis shown in figs. 7 and 8, the only ultraviolet pole is in the bubble integral.)

4.2. Unitarity

The conservation of probability is a fundamental requirement of any consistent field theory. It implies the unitarity of the scattering matrix S . If we examine the non-forward part of the scattering matrix, $T = -i(S - 1)$, unitarity implies that

$$-i(T - T^\dagger) = T^\dagger T. \quad (4.4)$$

The implicit sum on the right-hand side goes over all possible physical states, intermediate between the processes defined by T^\dagger and T . At one-loop order, only two-particle intermediate states are possible. There is a phase-space integral over the intermediate on-shell momenta, which amounts to an integral over the solid angle of one of the two particles, in the center-of-momentum frame. There is also a discrete sum over allowed particle types.

The left-hand side of eq. (4.4) corresponds to a discontinuity in the scattering amplitude, that is a branch cut in complex momenta. This discontinuity gives the absorptive part of an amplitude.

The right-hand side may be obtained from a loop amplitude by *cutting* it. In a single Feynman diagram, the discontinuity in a given invariant or channel can be computed by replacing the two propagators separating a set of legs carrying that invariant from the rest of the diagram by a delta function,

$$\frac{i}{p^2 + i\epsilon} \longrightarrow 2\pi \delta^{(+)}(p^2). \quad (4.5)$$

At the diagrammatic level, this replacement goes under the name of the Cutkosky rules [107]. The pair of delta functions reduces the loop integral to a phase-space integral. We can of course also cut sums of diagrams, taking care to throw away any contribution in which one or both of the required propagators is missing. (The missing propagator prevents such terms from contributing to the discontinuity in the target invariant.)

The application of unitarity as an on-shell method of calculation turns the cutting step around. Instead of cutting one-loop amplitudes, we will sew tree amplitudes together to form one-loop amplitudes. In other words, we will be reconstructing the dispersive parts of amplitudes from the absorptive ones. This reconstruction could in principle be accomplished by performing dispersion integrals; but we do *not* want to perform such integrals explicitly. Rather, we rely on the existence of an underlying representation in terms of Feynman integrals to do the job. For this purpose, we do not need an explicit basis of the kind discussed in the previous subsection, but having one makes the reconstruction easier and more powerful. In brief, we evaluate the cuts in each channel, and represent them as linear combinations of cuts of integrals \mathcal{I}_j in that channel,

$$\text{Im } A_n^{1\text{-loop}} = \sum_{j \in B} c_j \text{Im } \mathcal{I}_j, \quad (4.6)$$

in order to read off the coefficients c_j .

Consider the cut in a channel with momentum K crossing the cut, where K is composed of j external legs and $s = K^2$. The cut contains delta functions imposing the on-shell condition (4.5). By removing them, we promote the cut to a full loop integral,

$$\begin{aligned} (2\pi)^2 \sum_{\text{helicity}} \int \frac{d^D \ell}{(2\pi)^D} \delta^{(+)}(\ell^2) A_{n-j+2}^{\text{tree}}(K - \ell, \dots, \ell) \delta^{(+)}((\ell - K)^2) A_{j+2}^{\text{tree}}(-\ell, \dots, \ell - K) \\ \rightarrow \sum_{\text{helicity}} \int \frac{d^D \ell}{(2\pi)^D} \frac{i}{\ell^2} A_{n-j+2}^{\text{tree}}(K - \ell, \dots, \ell) \frac{i}{(\ell - K)^2} A_{j+2}^{\text{tree}}(-\ell, \dots, \ell - K). \end{aligned} \quad (4.7)$$

Here the tree amplitudes are on shell, and the sum is taken over the possible helicities of the internal legs crossing the cut. In the applications we will describe in this review, the cut momenta entering the tree amplitudes in eq. (4.7) are taken to be four-dimensional. Accordingly, we can use the spinor-helicity method to the fullest in evaluating them.

The propagators in eq. (4.7) are the same whether the particle crossing the cut is a scalar, a fermion, or a gauge boson. The corresponding helicity projector is already present in the on-shell tree amplitudes. The loop integral, in contrast, is evaluated in D dimensions. The integral reductions discussed in the previous subsection are algebraic manipulations of the integrand. To perform them on expressions given in terms of spinor products, we can complete the spinor products to form scalar-propagator denominators. For example, if external momentum k_1 appears right after the loop momentum ℓ , then we may write,

$$\frac{1}{\langle \ell k_1 \rangle} = -\frac{[\ell k_1]}{2\ell \cdot k_1} = \frac{[\ell k_1]}{(\ell - k_1)^2}. \quad (4.8)$$

If all denominators are converted to scalar propagators, then the numerators can be rewritten as functions of the loop momentum (and not merely of spinors carrying the on-shell cut loop momentum). Performing the integral reductions on this expression will decompose the integrand into a sum of terms, each corresponding to an integral in the basis eq. (4.3). We can then read off the coefficient of any integral from the term with propagators corresponding to the integral. In practice, applying the full reduction machinery is not necessary; appropriate partial-fractioning of the integrand with respect to the loop momentum accomplishes the same goal. As outlined below, an alternative approach for computing the coefficients, developed by Britto *et al.* [51,57], transforms the cut integral into a contour integral in spinor variables, which may be evaluated by residue extraction.

In a general amplitude, we cannot detect all terms by looking in a single channel. For this reason, we have to look at all channels. Some integrals contributing to the amplitude will appear only in a single channel; we can simply read off the coefficient in that channel. Other integrals will show up in more than one channel; we can read off their coefficients in any of the channels. We must take only a single copy of the integral in the latter case.

Within the basis used in eq. (4.3), cutting the amplitude in a given channel isolates those integrals that have a discontinuity in it. The product of tree amplitudes A_{n-j+2}^{tree} , A_{j+2}^{tree} can be equated to a linear combination of cuts of a subset of integrals in the basis,

as in eq. (4.6). Because the linear combination typically contains more than one integral, we have to identify the different terms on the left-hand side. One way to do this is by performing a partial-fraction decomposition, and then isolating different terms according to the propagators they contain. We will refine this isolation in the next subsection.

One might worry that were we to use a dispersion integral to perform this reconstruction, the results we found would suffer from an additive ambiguity because of ultraviolet divergences in the integral. That is, one can add a branch-cut-free or rational function to the amplitude. Such rational terms are indeed present in QCD amplitudes. They cannot be computed using the four-dimensional unitarity approach described above. In the four-dimensional case, the coefficients in the basis (4.3) are understood to have ϵ set to zero, and the basis only serves as one for the cut-containing parts of the amplitude.

As an aside, we note that in supersymmetric theories at one loop, rational terms are tightly linked to cut-containing terms. They can be deduced entirely from the integral functions determined within the four-dimensional approach. There are no missing terms. (In theories with $\mathcal{N} = 4$ supersymmetry, there are strong indications that the same result is even true at higher loops.) This result reflects the improved ultraviolet behavior of supersymmetric theories.

There are two distinct on-shell methods for computing these rational terms, implicitly fixing this remaining ambiguity. (For other analytic approaches, see refs. [40,41].) One method, to be discussed in section 5, is to extend on-shell methods by making use of another universal property of amplitudes, that of factorization.

The second method stretches slightly our notion of a physical state from four to D dimensions [46,58]. If we take the sum over intermediate states in D dimensions instead of four dimensions, we recover the entire amplitude with no rational ambiguity. These intermediate states are massless and transverse but in a D -dimensional rather than a four-dimensional sense. The latter method adds a third role to dimensional regularization, beyond regulating both ultraviolet and infrared divergences.

There are two different ways of understanding how D -dimensional unitarity can capture the complete amplitude. From the point of view of dispersion integrals, dimensional regularization makes the absorptive part of the amplitude ultraviolet convergent, and hence eliminates any additive ambiguity. From a more concrete point of view, every term in an amplitude must contain a power of $(-s)^{-\epsilon}$, where s is an invariant, in order to compensate the dimension of the coupling and keep the amplitude of fixed dimension as we change ϵ . (In an amplitude with only massless particles propagating internally, there are no masses to supply the required dimension.) The invariants s that appear can be different in different terms of the amplitude. If we now expand the amplitude beyond $\mathcal{O}(\epsilon^0)$, the epsilonic power $(-s)^{-\epsilon}$ will give rise to a term,

$$1 - \epsilon \ln(-s) + \cdots, \quad (4.9)$$

which contains a discontinuity for $s > 0$. Hence it will be detected in the unitarity cut in the s channel. The rational terms can then be obtained by truncating the result to $\mathcal{O}(\epsilon^0)$. The underlying Feynman-integral representation forces them to come along with the $\mathcal{O}(\epsilon)$ cut terms.

Because the D -dimensional unitarity method effectively computes the amplitude to all orders in ϵ , it goes beyond what is truly needed for collider applications. It does not allow full use of the spinor-helicity basis at the early stages of a calculation, though of course we can still make use of the on-shell conditions in D dimensions. Accordingly, it tends to

require more computational effort than the combination of the four-dimensional unitarity method with the additional techniques for rational parts discussed in section 5. Nonetheless it is conceptually useful, and can be useful in practice for lower-point amplitudes needed as starting points for the recursive techniques we review later. It is necessary to use this version of unitarity, of course, when one needs a quantity, such as a splitting amplitude, to higher order in ϵ . Recent work [58,60] has shown how to apply spinor methods in this context as well, and should widen the applicability of D -dimensional methods.

4.3. Generalized Unitarity

Cutting propagators in an amplitude selects only those contributions that have the propagators present in the first place. We can think of this in terms of the original Feynman diagrams for our target amplitude, where it reflects the observation that a diagram with a relevant propagator missing cannot contribute to the discontinuity in the desired channel. We can also think of this in terms of the integrals in the basis. Each original Feynman diagram will produce contributions to the coefficients of several basis integrals. If the original diagram is missing a required propagator, none of the corresponding basis integrals will have it, and no contribution to the discontinuity will arise. Even when the original diagram does have a required propagator, it will be present only in a subset of the descendant basis integrals. Cutting pairs of propagators thus winnows the set of basis integrals down to those in which the pair is present. When we sew together two tree amplitudes to form the cut in a given channel, only those integrals that possess both cut propagators can show up in the result, and accordingly the given cut contributes only to the coefficients of those integrals.

As discussed in the previous subsection, we must in general perform analytic simplifications on the cut expression in order to isolate the contributions of different integrals. This procedure will sort terms into contributions corresponding to different integrals according to the propagator denominators present, and will remove contributions to lower-point integrals. If we require the presence of additional propagators beyond the pair isolating a given channel, only a subset of terms will remain. That is, fewer integrals can contribute. Requiring the presence of additional propagators, or equivalently cutting them, goes under the name of ‘generalized unitarity’. It corresponds, in the old-fashioned language of dispersion relations, to extracting the leading discontinuity of an amplitude [108]. In addition to isolating a smaller number of candidate integrals to consider, the additional on-shell condition splits one of the two tree amplitudes into smaller trees. We are thus sewing smaller and simpler expressions together, and will in general need to perform less algebra to extract coefficients.

The ultimate refinement of this procedure comes when we require enough propagators to isolate a *single* integral. This is possible for the box integrals. Maximal generalized unitarity — cutting four propagators — isolates the coefficient of a single box integral as a product of four tree amplitudes, as illustrated in fig. 1(b). In addition, when we take the cut momenta to be strictly four-dimensional, the four delta functions freeze the loop momentum entirely [49],

$$\int \frac{d^D \ell}{(2\pi)^D} \left[\frac{f(\ell)}{[\ell^2 + i\epsilon][(\ell - K_1)^2 + i\epsilon][(\ell - K_{12})^2 + i\epsilon][(\ell - K_{123})^2 + i\epsilon]} \right] \Big|_{\ell^D \rightarrow \ell^4}$$

$$\begin{aligned}
&\longrightarrow \int \frac{d^D \ell}{(2\pi)^D} [f(\ell) \delta^{(+)}(\ell^2) \delta^{(+)}((\ell - K_1)^2) \delta^{(+)}((\ell - K_{12})^2) \delta^{(+)}((\ell - K_{123})^2)] \Big|_{\ell^D \rightarrow \ell^4} \\
&= \frac{1}{2} \sum_{\text{solutions}} f(\ell).
\end{aligned} \tag{4.10}$$

The sum is over the discrete number of solutions to the simultaneous on-shell equations imposed by the four-dimensional delta functions. The coefficient of the desired integral is then simply the product of the four tree amplitudes, summed over these solutions for the cut loop momenta $\ell^{(m)}$,

$$\begin{aligned}
c_j = \frac{1}{2} \sum_{m=1,2} & A_{n_1}^{\text{tree}}(\dots, -\ell^{(m)}, \ell^{(m)} - K_1, \dots) A_{n_2}^{\text{tree}}(\dots, -\ell^{(m)} + K_1, \ell^{(m)} - K_{12}, \dots) \\
& \times A_{n_3}^{\text{tree}}(\dots, -\ell^{(m)} + K_{12}, \ell^{(m)} - K_{123}, \dots) A_{n_4}^{\text{tree}}(\dots, -\ell^{(m)} + K_{123}, \ell^{(m)}, \dots),
\end{aligned} \tag{4.11}$$

where the implicit momenta are all external, and $\sum_i n_i = n + 8$. The sum is normalized by the total number of solutions, which turns out to be two, including solutions for which f may happen to vanish. The complete freezing of the loop momentum means that no further algebra is required, and the coefficient could even be evaluated purely numerically.

For many applications of eq. (4.11), including all for less than eight external (massless) legs, there would seem to be a catch: some of the tree amplitudes, corresponding to massless external legs, will be all-massless three-point amplitudes. Naively, these amplitudes would vanish. The quadruple cuts would vanish along with them, swallowing the coefficients with them. As we have seen in section 2, however, using complex momenta we can obtain non-zero values for these amplitudes. We can then treat them in the same way as higher-point amplitudes in the quadruple cuts, and recover the box coefficients simply from sums over appropriate products of tree amplitudes. Indeed, as we shall see, because of the special properties of three-point amplitudes, the computation of coefficients of box integrals with massless external legs is even simpler than that of four-mass boxes.

In an approach based on maximal use of generalized unitarity, we will compute a larger number of cuts; but each cut will be simpler, and will give the coefficient of a single integral directly. One starts with the box integrals, computing a separate quadruple cut for each different one. One turns next to the three-mass triangles, which can be isolated through triple cuts as was done in ref. [64]. The integrands emerging from triple cuts in general will also contain contributions to those box integrals sharing the same cuts. These contributions, and box-like terms which vanish upon loop integration, must be removed in order to extract the coefficient of the three-mass triangle. This can be done, for example, using the decomposition proposed by Ossola *et al.* [42], or by other methods. Further developments here are possible and desirable (see *e.g.* ref. [69]). The spinor-residue approach of refs. [51,57] outlined below can also be used for this evaluation. The remaining terms come from one- and two-mass triangles as well as bubble integrals. The analytic forms of the one- and two-mass triangle integrals imply that the remaining terms can all be written as sums of bubble integrals, with coefficients that depend on external invariants and on ϵ . Accordingly, they should be treated together. This part of the computation will make use of standard cuts, evaluated as described in the previous section 4.2.

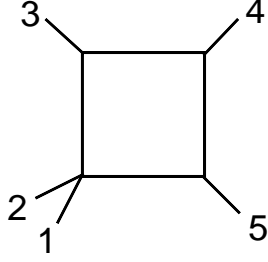


Fig. 9. A box integral that can occur for five-point amplitudes with legs following the 12345 ordering. The other four possible ones are given by cyclic permutations of this one.

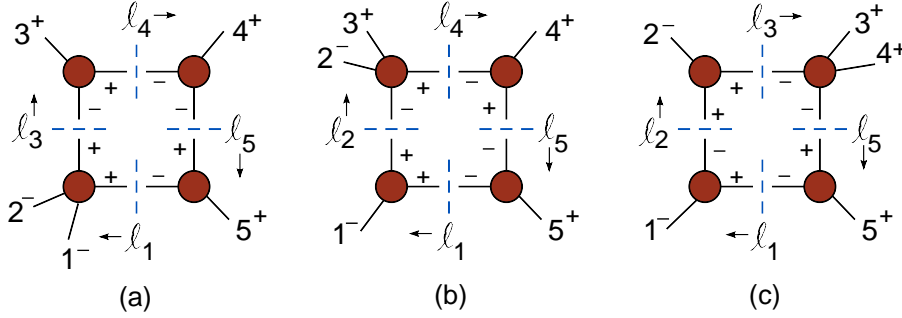


Fig. 10. The quadruple cuts of of integrals $\mathcal{I}(K_{12})$, $\mathcal{I}(K_{23})$, and $\mathcal{I}(K_{34})$. Only one helicity configuration contributes to each of the cuts.

4.4. A Box Example

As an example, let us compute the coefficient of a box integral in the pure gauge-theory amplitude $A_5^{1\text{-loop}}(1^-, 2^-, 3^+, 4^+, 5^+)$. Because this amplitude contains five external massless legs, the relevant box integrals, which are found by collapsing a single propagator on the pentagon ring diagram, have precisely one external massive leg, and three massless ones. One of these one-mass box integrals, in which the massive leg is $K_{12} = k_1 + k_2$, is shown in fig. 9. It is defined by

$$\mathcal{I}(K_{12}) = \mu^{2\epsilon} \int \frac{d^{4-2\epsilon} \ell}{(2\pi)^{4-2\epsilon}} \frac{1}{\ell^2 (\ell - K_{12})^2 (\ell - K_{123})^2 (\ell + k_5)^2}. \quad (4.12)$$

The other four boxes have the massive leg in turn being K_{23} , K_{34} , K_{45} and K_{51} . The amplitude $A_5^{1\text{-loop}}(1^-, 2^-, 3^+, 4^+, 5^+)$ is antisymmetric under the reflection $(12345) \leftrightarrow (21543)$. This symmetry relates the coefficient of $\mathcal{I}(K_{51})$ to that of $\mathcal{I}(K_{23})$; and that of $\mathcal{I}(K_{45})$ to that of $\mathcal{I}(K_{34})$.

Let us perform the computation for $\mathcal{I}(K_{12})$, using maximal generalized unitarity. When we cut all four propagators, as shown in fig. 10(a), and restrict the cut momenta to four dimensions, we will be left with three three-point amplitudes and one four-point amplitude. If ℓ_4 is the cut loop momentum in between k_3 and k_4 , it is a momentum entering into both adjacent three-vertices. In order to obtain a nonvanishing result, we must take it to be complex. The on-shell conditions on the first vertex require that

$$\text{either } \lambda_{\ell_4} \propto \lambda_3 \quad \text{or} \quad \tilde{\lambda}_{\ell_4} \propto \tilde{\lambda}_3, \quad (4.13)$$

and the on-shell conditions on the second vertex require that

$$\text{either } \lambda_{\ell_4} \propto \lambda_4 \quad \text{or} \quad \tilde{\lambda}_{\ell_4} \propto \tilde{\lambda}_4. \quad (4.14)$$

However, for generic external momenta, $s_{34} \neq 0$, and therefore $\lambda_3 \not\propto \lambda_4$ and $\tilde{\lambda}_3 \not\propto \tilde{\lambda}_4$. Thus only two of the combined solutions are allowed,

$$(\lambda_{\ell_4} \propto \lambda_3 \text{ and } \tilde{\lambda}_{\ell_4} \propto \tilde{\lambda}_4) \quad \text{or} \quad (\tilde{\lambda}_{\ell_4} \propto \tilde{\lambda}_3 \text{ and } \lambda_{\ell_4} \propto \lambda_4). \quad (4.15)$$

This in turn implies that neighboring three-vertices must be of opposite ‘type’ — if one is of the form $A_3^{\text{tree}}(+ + -)$ or a cyclic permutation thereof, then its neighbor must be of the form $A_3^{\text{tree}}(- - +)$ or a cyclic permutation thereof.

The possible helicity configurations are further restricted by the identity of the helicities attached to the massive leg. The vanishing of four-point tree amplitudes with zero or one positive helicity (the parity conjugate of eq. (2.26)) implies that the helicities of both cut internal legs emerging from the four-point vertex, $(-\ell_1)$ and ℓ_3 , must be positive. Such a configuration is only allowed for gluonic internal states; it vanishes for quarks or scalars circulating in the loop. (Massless fermions have their helicity conserved along the fermion line, which translates into a helicity flip between quark and anti-quark legs, in our all-outgoing helicity convention. Scalars do not carry helicity, but they can be considered to be complex, and then particle *vs.* anti-particle plays the same role as helicity.) The positive helicity of $(-\ell_1)$ and ℓ_3 , together with the neighboring-three-vertex constraint, fixes the helicities of the remaining three-point vertices to be $A_3^{\text{tree}}(-\ell_3^-, 3^+, \ell_4^+)$, $A_3^{\text{tree}}(-\ell_4^-, 4^+, \ell_5^-)$, and $A_3^{\text{tree}}(-\ell_5^+, 5^+, \ell_1^-)$. Accordingly, we have only a single solution, the first in eq. (4.15), to take into account. The other solution leads to vanishing three-point tree amplitudes, as discussed in section 2.

To evaluate the coefficient, we must solve for ℓ_4 . We only need the solutions for λ_{ℓ_4} and $\tilde{\lambda}_{\ell_4}$ up to an overall constant factor, because the latter will cancel in the combination that appears in the desired coefficient, $\lambda_{\ell_4} \tilde{\lambda}_{\ell_4}$. Three of the four on-shell equations,

$$\ell_4^2 = 0, \quad \ell_3^2 = (\ell_4 + k_3)^2 = 0, \quad \text{and} \quad \ell_5^2 = (\ell_4 - k_4)^2 = 0, \quad (4.16)$$

can be satisfied automatically by taking ℓ_4^μ to have the form,

$$\ell_4^\mu = \frac{1}{2} \xi_4 \langle 3^- | \gamma^\mu | 4^- \rangle. \quad (4.17)$$

The constant ξ_4 is fixed by the last of the four on-shell equations,

$$\ell_1^2 = (\ell_4 - K_{45})^2 = -\xi_4 \langle 3^- | 5 | 4^- \rangle + s_{45} = 0, \quad (4.18)$$

to have the value $\xi_4 = \langle 45 \rangle / \langle 35 \rangle$.

The coefficient of the K_{12} box is then,

$$\begin{aligned} c_{12} &= \frac{1}{2} A_4^{\text{tree}}(-\ell_1^+, 1^-, 2^-, \ell_3^+) A_3^{\text{tree}}(-\ell_3^-, 3^+, \ell_4^+) A_3^{\text{tree}}(-\ell_4^-, 4^+, \ell_5^-) A_3^{\text{tree}}(-\ell_5^+, 5^+, \ell_1^-) \\ &= \frac{1}{2} \frac{\langle 12 \rangle^3}{\langle 2\ell_3 \rangle \langle \ell_3(-\ell_1) \rangle \langle (-\ell_1)1 \rangle} \frac{[3\ell_4]^3}{[\ell_4(-\ell_3)] [(-\ell_3)3]} \frac{\langle \ell_5(-\ell_4) \rangle^3}{\langle 4\ell_5 \rangle \langle (-\ell_4)4 \rangle} \frac{[(-\ell_5)5]^3}{[5\ell_1] [\ell_1(-\ell_5)]} \\ &= -\frac{1}{2} \frac{\langle 12 \rangle^3 \langle 3^+ | \ell_4 \ell_5 | 5^- \rangle^3}{\langle 2^- | \ell_3 | 3^- \rangle \langle 4^- | \ell_4 \ell_3 \ell_1 | 5^- \rangle \langle 1^- | \ell_1 \ell_5 | 4^+ \rangle}. \end{aligned} \quad (4.19)$$

Using momentum conservation and the properties of the ℓ_i , we can simplify this expression to,

$$\begin{aligned}
c_{12} &= \frac{1}{2} \frac{\langle 12 \rangle^3 \langle 4^- | \ell_4 | 3^- \rangle^2 [45]^3}{\langle 2^- | \ell_4 | 3^- \rangle \langle 34 \rangle [45] \langle 15 \rangle \langle 4^- | \ell_4 | 5^- \rangle} \\
&= -\frac{1}{2} \frac{\langle 12 \rangle^3 s_{34} s_{45}}{\langle 23 \rangle \langle 34 \rangle \langle 45 \rangle \langle 51 \rangle} \\
&= \frac{i}{2} s_{34} s_{45} A_5^{\text{tree}}(1^-, 2^-, 3^+, 4^+, 5^+). \tag{4.20}
\end{aligned}$$

The box integral multiplying this coefficient, defined in eq. (4.12), has the Laurent expansion in ϵ ,

$$\begin{aligned}
\mathcal{I}(K_{12}) &= \frac{-2i c_\Gamma}{s_{34} s_{45}} \left\{ -\frac{1}{\epsilon^2} \left[\left(\frac{\mu^2}{-s_{34}} \right)^\epsilon + \left(\frac{\mu^2}{-s_{45}} \right)^\epsilon - \left(\frac{\mu^2}{-s_{12}} \right)^\epsilon \right] \right. \\
&\quad \left. + \text{Li}_2 \left(1 - \frac{s_{12}}{s_{34}} \right) + \text{Li}_2 \left(1 - \frac{s_{12}}{s_{45}} \right) + \frac{1}{2} \ln^2 \left(\frac{-s_{34}}{-s_{45}} \right) + \frac{\pi^2}{6} \right\} \\
&\quad + \mathcal{O}(\epsilon), \tag{4.21}
\end{aligned}$$

where the constant c_Γ is defined by

$$c_\Gamma = \frac{1}{(4\pi)^{2-\epsilon}} \frac{\Gamma(1+\epsilon)\Gamma^2(1-\epsilon)}{\Gamma(1-2\epsilon)}. \tag{4.22}$$

The coefficients of the other boxes also have only gluonic contributions. In the K_{23} box, shown in fig. 10(b), the four-point vertex has opposite helicities for the internal legs; but the requirement of opposite ‘type’ for adjacent three-point vertices requires the diagonally-opposite three-point vertex to have identical helicities for its internal momenta. This allows only gluonic contributions. In the K_{34} box, both internal legs attached to the four-point vertex containing k_3 and k_4 have identical helicity, again allowing only gluonic contributions as shown in fig. 10(c). An explicit computation shows that the coefficients of these two boxes are in fact similar to the coefficient of the K_{12} box (4.20); they are equal to the tree amplitude multiplied by the same constant and corresponding invariants ($is_{45}s_{51}/2$ for $\mathcal{I}(K_{23})$ and $is_{51}s_{12}/2$ for $\mathcal{I}(K_{34})$). The gluon-loop contribution to the amplitude is then given by,

$$\begin{aligned}
A_5^{1\text{-loop}}(1^-, 2^-, 3^+, 4^+, 5^+) &= A_5^{\text{tree}}(1^-, 2^-, 3^+, 4^+, 5^+) c_\Gamma \left\{ \right. \\
&\quad -\frac{1}{\epsilon^2} \left[\left(\frac{\mu^2}{-s_{34}} \right)^\epsilon + \left(\frac{\mu^2}{-s_{45}} \right)^\epsilon - \left(\frac{\mu^2}{-s_{12}} \right)^\epsilon \right] \\
&\quad + \text{Li}_2 \left(1 - \frac{s_{12}}{s_{34}} \right) + \text{Li}_2 \left(1 - \frac{s_{12}}{s_{45}} \right) + \frac{1}{2} \ln^2 \left(\frac{-s_{34}}{-s_{45}} \right) + \frac{\pi^2}{6} \\
&\quad \left. + \text{cyclic permutations} \right\} + \text{triangles} + \text{bubbles}. \tag{4.23}
\end{aligned}$$

Next we discuss how to evaluate triangle and bubble contributions.

4.5. A Triangle Example

In a five-point amplitude with all external legs massless, three-mass triangles cannot arise. The remaining terms in the five-gluon amplitude are derived from one- or two-mass triangles in addition to bubble integrals. These integrals can be expressed as,

$$\mathcal{I}_2(s) = \frac{i c_\Gamma}{\epsilon(1-2\epsilon)} \left(\frac{\mu^2}{-s} \right)^\epsilon, \quad (4.24)$$

$$\mathcal{I}_3^{1m}(s) = -\frac{i c_\Gamma}{\epsilon^2} \left(\frac{\mu^2}{-s} \right)^\epsilon, \quad (4.25)$$

$$\mathcal{I}_3^{2m}(s_1, s_2) = -\frac{\mathcal{I}_3^{1m}(s_1) - \mathcal{I}_3^{1m}(s_2)}{s_1 - s_2}. \quad (4.26)$$

That is, they are all linear combinations of bubble integrals. Laurent expanding these expressions in ϵ , we see that all remaining terms at order ϵ^0 will consist either of logarithms or logarithms squared. As an example, we will compute the coefficient of one of the logarithms in the internal-scalar contributions to the amplitude $A_5^{1\text{-loop}}(1^-, 2^-, 3^+, 4^+, 5^+)$. These terms will be required in our recursive computation of the rational terms in section 5.

To compute these terms, we can proceed in a variety of ways. In order to detect bubble integrals, we must in any event include ordinary cuts, which enforce the presence of just two propagators. We would proceed, for example, by forming the ordinary cut in each of the three distinct channels — s_{12} , s_{23} , and s_{34} . Various box integrals also have cuts in these channels, so we would have to subtract their contributions to the integrand. What is left will give us the remaining logarithms. In the internal-scalar example we are considering, this approach is particularly simple, because as discussed above the scalar and fermionic contributions have no box integrals, and hence there is nothing to subtract. (In principle, there could be contributions that integrate to zero, requiring a nontrivial subtraction, but that does not happen here.)

Helicity conservation also means that in both scalar and fermionic contributions, the internal lines emerging from each tree amplitude must have opposite helicities. Therefore the cuts in the s_{12} , s_{34} , and s_{45} channels will vanish, because the resulting four-point amplitudes will have the helicity structure $(- + + +)$, and the corresponding tree amplitudes all vanish. We are left with contributions only in the s_{23} and s_{51} channels. We will compute the coefficient of $\ln(-s_{23})$; the coefficient of $\ln(-s_{51})$ is related by the reflection symmetry $(12345) \leftrightarrow (21543)$. In this particular amplitude, the triangles generate no squared logarithms.

The scalar contribution to the s_{23} cut is,

$$\begin{aligned} & \sum_{h=\pm} A_4^{\text{tree}}(-\ell_{2s}^h, 2^-, 3^+, \ell_{4s}^{-h}) A_5^{\text{tree}}(-\ell_{4s}^h, 4^+, 5^+, 1^-, \ell_{2s}^{-h}) \\ &= -2 \frac{\langle (-\ell_2) 2 \rangle^2 \langle \ell_4 2 \rangle^2 \langle (-\ell_4) 1 \rangle^2 \langle \ell_2 1 \rangle^2}{\langle (-\ell_2) 2 \rangle \langle 2 3 \rangle \langle 3 \ell_4 \rangle \langle \ell_4 (-\ell_2) \rangle \langle \ell_2 (-\ell_4) \rangle \langle (-\ell_4) 4 \rangle \langle 4 5 \rangle \langle 5 1 \rangle \langle 1 \ell_2 \rangle} \\ &= 2 \frac{\langle \ell_4 1 \rangle \langle \ell_4 2 \rangle \langle 2^- | K_{23} \ell_4 | 1^+ \rangle \langle 2^- | \ell_4 K_{23} | 1^+ \rangle}{\langle 2 3 \rangle \langle 3 \ell_4 \rangle s_{23}^2 \langle \ell_4 4 \rangle \langle 4 5 \rangle \langle 5 1 \rangle}. \end{aligned} \quad (4.27)$$

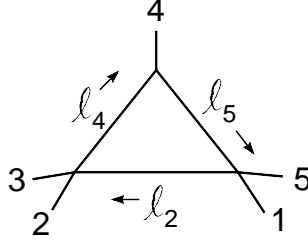


Fig. 11. The two-mass triangle arising from the second term in eq. (4.29).

(The ‘helicity’ label for a scalar distinguishes particle and antiparticle, which give equal contributions.)

We can separate the ℓ_4 -dependent denominators, using the Schouten identity,

$$\langle \ell_4 1 \rangle \langle 3 4 \rangle = \langle \ell_4 3 \rangle \langle 1 4 \rangle + \langle \ell_4 4 \rangle \langle 3 1 \rangle, \quad (4.28)$$

as a kind of partial-fraction decomposition. We get,

$$\frac{\langle \ell_4 1 \rangle \langle \ell_4 2 \rangle}{\langle 3 \ell_4 \rangle \langle \ell_4 4 \rangle} = \frac{1}{\langle 3 4 \rangle} \left(\frac{\langle 1 3 \rangle \langle 2^- | \ell_4 | 3^- \rangle}{(\ell_4 + k_3)^2} + \frac{\langle 1 4 \rangle \langle 2^- | \ell_4 | 4^- \rangle}{(\ell_4 - k_4)^2} \right). \quad (4.29)$$

Each term now corresponds to a different triangle integral, the first to a one-mass one and the second to a two-mass one. Both still have non-trivial numerators. The one-mass triangle turns out to give a vanishing contribution to our amplitude.

The two-mass triangle integral depicted in fig. 11, coming from the second term in eq. (4.29), has the form,

$$2 \frac{\langle 1 4 \rangle}{\langle 2 3 \rangle \langle 3 4 \rangle \langle 4 5 \rangle \langle 5 1 \rangle s_{23}^2} \times \int \frac{d^{4-2\epsilon} \ell}{(2\pi)^{4-2\epsilon}} \frac{\langle 2^- | \ell_4 | 4^- \rangle \langle 2^- | K_{23} \ell_4 | 1^+ \rangle \langle 2^- | \ell_4 K_{23} | 1^+ \rangle}{\ell_2^2 \ell_4^2 \ell_5^2}. \quad (4.30)$$

Here, and below, the ℓ_i are taken to be off-shell loop momenta corresponding to the cut momenta denoted by the same variables above. We can expand the loop momenta in the numerator of eq. (4.30) as discussed in section 4.1, using the basis in eq. (4.2): two real vectors, $v_1^\mu = K_{23}^\mu$ and $v_2^\mu = K_{51}^\mu$, as well as two complex vectors, $v_3^\mu = \langle 4^+ | K_{23} \gamma^\mu | 4^- \rangle$ and $v_4^\mu = \langle 4^- | K_{23} \gamma^\mu | 4^+ \rangle$. This choice is convenient, because powers of these two complex vectors will give rise to vanishing integrals [42]. It generalizes in a straightforward way to processes beyond the five-point example considered here. In terms of the v_i basis, the loop momentum expansion is,

$$\begin{aligned} \ell_4^\mu = & - \left[\frac{(\ell_4 + K_{23})^2 - s_{23}}{s_{51} - s_{23}} + \frac{s_{51} + s_{23}}{(s_{51} - s_{23})^2} (\ell_4 - k_4)^2 \right] v_1^\mu \\ & - \left[\frac{(\ell_4 + K_{23})^2 - s_{23}}{s_{51} - s_{23}} + 2 \frac{s_{23}}{(s_{51} - s_{23})^2} (\ell_4 - k_4)^2 \right] v_2^\mu \\ & + \frac{1}{2(s_{51} - s_{23})^2} \langle 4^- | K_{23} \ell_4 | 4^+ \rangle v_3^\mu + \frac{1}{2(s_{51} - s_{23})^2} \langle 4^+ | K_{23} \ell_4 | 4^- \rangle v_4^\mu. \end{aligned} \quad (4.31)$$

Referring to fig. 11, we see that the factor $(\ell_4 + K_{23})^2 = \ell_2^2$ will cancel a denominator, leaving a bubble integral with a massless leg, which vanishes in dimensional regularization. We can therefore drop such terms. A factor of $(\ell_4 - k_4)^2 = \ell_5^2$ will also cancel a propagator, leaving a bubble with external momentum K_{23} . It may contribute to the coefficient of the logarithm we are computing.

After substituting this form for ℓ_4 into the numerator of the integrand, we will obtain terms leading to integrals in the classes,

$$\mathcal{I}_3[(\ell_4 \cdot v_3)^{a_3} (\ell_4 \cdot v_4)^{a_4}] \quad \text{and} \quad \mathcal{I}_2[(\ell_4 \cdot k_4)^{a_1} (\ell_4 \cdot v_3)^{a_3} (\ell_4 \cdot v_4)^{a_4}]. \quad (4.32)$$

The underlying tensor integrals can be expressed in terms of the metric $g^{\mu\nu}$ and either $v_{1,2}^\mu$ in the three-point case, or v_1^μ alone in the two-point case. Because v_3 and v_4 are null vectors, and moreover $v_1 \cdot v_{3,4} = v_2 \cdot v_{3,4} = 0$, pure powers of either $\ell_4 \cdot v_3$ or $\ell_4 \cdot v_4$ in the three-point case ($a_4 = 0$ or $a_3 = 0$), or pure powers of them with $\ell_4 \cdot v_1$ (for any value of a_1), will yield vanishing integrals. Such numerator factors in a sense produce total derivatives, and thereby give an explicit realization of the vanishing integrals introduced in ref. [42]. We can use an identity,

$$\begin{aligned} \langle 4^+ | K_{23} \ell_4 | 4^- \rangle \langle 4^- | K_{23} \ell_4 | 4^+ \rangle &= (\ell_4 - k_4)^2 \times \frac{1}{2} \text{tr}[k_4 K_{23} \ell_4 K_{23}] \\ &= (\ell_4 - k_4)^2 \left[(s_{51} - s_{23})((\ell_4 + K_{23})^2 - s_{23}) - 2s_{23} \ell_4 \cdot k_4 \right], \end{aligned} \quad (4.33)$$

to eliminate mixed powers of the numerator factors ($a_3 \neq 0 \neq a_4$). Only equal powers, $a_3 = a_4$, will give a nonvanishing contribution.

We can thus derive the following replacement rules for the integrand,

$$\begin{aligned} \ell_4^\mu &\rightarrow v_+^\mu \equiv \frac{s_{23}(v_1^\mu + v_2^\mu)}{s_{51} - s_{23}} - \frac{s_{51}v_1^\mu + s_{23}(v_1^\mu + 2v_2^\mu)}{(s_{51} - s_{23})^2} (\ell_4 - k_4)^2 \\ \ell_4^\mu \ell_4^\nu &\rightarrow v_+^\mu v_+^\nu - \frac{s_{23}(\ell_4 - k_4)^2}{4(s_{51} - s_{23})^4} (s_{51} - s_{23} + 2\ell_4 \cdot k_4) (v_3^\mu v_4^\nu + v_4^\mu v_3^\nu) \\ \ell_4^\mu \ell_4^\nu \ell_4^\rho &\rightarrow v_+^\mu v_+^\nu v_+^\rho - \frac{s_{23}(\ell_4 - k_4)^2}{4(s_{51} - s_{23})^4} (s_{51} - s_{23} + 2\ell_4 \cdot k_4) \\ &\quad \times (v_3^\mu v_4^\nu v_+^\rho + \text{permutations of } (\mu, \nu, \rho)) \end{aligned} \quad (4.34)$$

Only terms without factors of $2\ell_4 \cdot k_4 = -(\ell_4 - k_4)^2$ can produce a two-mass triangle. These terms come from the replacement $\ell_4^\mu \rightarrow c(v_1 + v_2)^\mu = -ck_4^\mu$, which makes the integrand in eq. (4.30) vanish. We are left only with bubble integrals. We can think of these replacements as an explicit realization of the reductions introduced in ref. [35].

To evaluate these terms, we can use the following little table,

$$\begin{aligned} \mathcal{I}_2[\ell_4^\mu](s_{23}) &= -\frac{1}{2} K_{23}^\mu \mathcal{I}_2(s_{23}), \\ \mathcal{I}_2[\ell_4^\mu \ell_4^\nu](s_{23}) &= -\frac{1}{4(D-1)} s_{23} g^{\mu\nu} \mathcal{I}_2(s_{23}) + \frac{D}{4(D-1)} K_{23}^\mu K_{23}^\nu \mathcal{I}_2(s_{23}), \end{aligned} \quad (4.35)$$

which are the only tensor reductions we need to perform explicitly. The bubble integral itself is, from eq. (4.24),

$$\mathcal{I}_2(s_{23}) = i c_\Gamma \left(\frac{1}{\epsilon} + \ln \left(\frac{\mu^2}{-s_{23}} \right) - 2 \right) + \mathcal{O}(\epsilon). \quad (4.36)$$

The singular parts can also be extracted from the cuts. We will include them in the full cut part below. The rational part we will not include, because as explained in prior subsections, additional information beyond the four-dimensional cuts is required to compute the finite rational terms fully. The metric term will drop out when evaluating integrals with numerator powers of $\ell_4 \cdot k_4$, so that in our computation we are left with,

$$\begin{aligned} \mathcal{I}_2[2\ell_4 \cdot k_4](s_{23}) &= \frac{1}{2}(s_{23} - s_{51}) \mathcal{I}_2(s_{23}), \\ \mathcal{I}_2[(2\ell_4 \cdot k_4)^2](s_{23}) &= \frac{D}{4(D-1)}(s_{23} - s_{51})^2 \mathcal{I}_2(s_{23}). \end{aligned} \quad (4.37)$$

Using these values, the terms containing cuts in the s_{23} channel are,

$$\begin{aligned} & -\frac{i c_\Gamma}{6} \frac{1}{\langle 23 \rangle \langle 34 \rangle \langle 45 \rangle \langle 51 \rangle} \ln \left(\frac{-s_{23}}{\mu^2} \right) \\ & \times \left(2 \frac{\langle 23 \rangle [34] \langle 41 \rangle \langle 24 \rangle [45] \langle 51 \rangle B}{(s_{51} - s_{23})^3} - \frac{\langle 12 \rangle^2 B}{s_{51} - s_{23}} + \langle 12 \rangle^3 \right). \end{aligned} \quad (4.38)$$

in which $B = \langle 23 \rangle [34] \langle 41 \rangle + \langle 24 \rangle [45] \langle 51 \rangle$.

Most of the factors appearing in the denominators, along with the factors in the denominator in eq. (4.20), are nearest-neighbor spinor products. These correspond to genuine physical singularities of the one-loop amplitude: as at tree level, their vanishing corresponds to a collinear limit. The $s_{51} - s_{23}$ and $(s_{51} - s_{23})^3$ denominators do not correspond to such physical singularities, and as such cannot be present in the amplitude. The singularity in the cut-containing terms is canceled by the contribution from the s_{51} channel, which is related by the flip symmetry $(12345) \leftrightarrow (21543)$. It combines with the expression in eq. (4.38) via the replacement,

$$\ln \left(\frac{-s_{23}}{\mu^2} \right) \longrightarrow \ln \left(\frac{-s_{23}}{-s_{51}} \right). \quad (4.39)$$

The logarithms in these contributions thus show up in the following functional forms containing spurious singularities,

$$\frac{\ln r}{1-r} \quad \text{and} \quad \frac{\ln r}{(1-r)^3}, \quad (4.40)$$

where r is the ratio of two momentum invariants. The singularity in these functions as $r \rightarrow 1$ is purely rational,

$$\begin{aligned} \frac{\ln r}{1-r} &\sim -1 + \frac{r-1}{2} - \frac{(r-1)^2}{3} + \dots, \\ \frac{\ln r}{(1-r)^3} &\sim -\frac{1}{(r-1)^2} + \frac{1}{2(r-1)} - \frac{1}{3} + \dots. \end{aligned} \quad (4.41)$$

The remaining singular terms must therefore be canceled by rational terms. We show how to compute these terms in the next section. It will be convenient, however, to anticipate the cancellation, and to define new functions which are manifestly free of spurious singularities,

$$\begin{aligned}
L_0(r) &= \frac{\ln r}{1-r}, \\
L_1(r) &= \frac{\ln r + 1 - r}{(1-r)^2}, \\
L_2(r) &= \frac{\ln r - (r - 1/r)/2}{(1-r)^3}.
\end{aligned} \tag{4.42}$$

We can now assemble the complete cut-containing terms for the internal-scalar contributions to $A_5^{1\text{-loop}}(1^-, 2^-, 3^+, 4^+, 5^+)$,

$$\begin{aligned}
&A_5^{\text{scalar}}(1^-, 2^-, 3^+, 4^+, 5^+)|_{\text{cut-containing}} = \\
&i c_{\Gamma} \left\{ \frac{\langle 12 \rangle^3}{6 \langle 23 \rangle \langle 34 \rangle \langle 45 \rangle \langle 51 \rangle} \left[\frac{2}{\epsilon} - \ln \left(\frac{-s_{23}}{\mu^2} \right) - \ln \left(\frac{-s_{51}}{\mu^2} \right) \right] \right. \\
&\quad - \frac{1}{3 \langle 23 \rangle \langle 34 \rangle \langle 45 \rangle \langle 51 \rangle} \\
&\quad \left. \times \left[\frac{\langle 23 \rangle [34] \langle 41 \rangle \langle 24 \rangle [45] \langle 51 \rangle B L_2 \left(\frac{-s_{23}}{-s_{51}} \right)}{s_{51}^3} - \frac{\langle 12 \rangle^2 B L_0 \left(\frac{-s_{23}}{-s_{51}} \right)}{2s_{51}} \right] \right\}. \tag{4.43}
\end{aligned}$$

The simplifications due to the choice of basis used here in the evaluation of two-mass triangle contributions should generalize to other amplitudes. Using the bases given in eqs. (4.1) and (4.2), we will obtain replacements similar to those given in eq. (4.34).

4.6. A Spinorial Approach

The above example illustrates how triangle and bubble integral coefficients can be evaluated in an ordinary two-particle cut using projections and vanishing integrals [35,42]. For more complicated cases, it is useful to have a systematic procedure that still keeps the analytic expressions relatively compact. (Feynman parametrization of cut loop integrals, for example, is a systematic method, but it tends to generate an explosion of terms.) In refs. [51,57], Britto *et al.* used spinorial variables in an efficient and systematic technique for evaluating generic one-loop unitarity cuts. The cut integration is effectively performed by residue extraction. Applying these ideas, they computed the cut-containing terms for the most complicated of the six-gluon helicity amplitudes with a scalar or fermion circulating in the loop.

This method makes use of an elegant decomposition of phase-space integrals in terms of spinor variables [93],

$$\int d^4 \ell \delta^{(+)}(\ell^2) f(\ell) = \int_0^\infty t dt \int \langle \ell d\ell \rangle [\ell d\ell] f(\ell), \tag{4.44}$$

where $\langle \ell d\ell \rangle \equiv \varepsilon^{\alpha\beta}(\lambda_\ell)_\alpha (d\lambda_\ell)_\beta$, $[\ell d\ell] \equiv \varepsilon^{\dot{\alpha}\dot{\beta}}(\tilde{\lambda}_\ell)_{\dot{\alpha}} (d\tilde{\lambda}_\ell)_{\dot{\beta}}$ and $\ell_\mu = t \langle \ell^- | \gamma_\mu | \ell^- \rangle / 2$. On the contour of integration λ_ℓ and $\tilde{\lambda}_\ell$ should be treated as complex conjugate variables, although elsewhere in this review we treat them as independent.

In a two-particle cut, this decomposition gives,

$$\begin{aligned}
C_2 &= \int d^4\ell \delta^{(+)}(\ell^2) \delta^{(+)}((\ell - K)^2) f(\lambda_\ell, \tilde{\lambda}_\ell, t) \\
&= \int_0^\infty t dt \int \langle \ell d\ell \rangle [\ell d\ell] \delta^{(+)}(K^2 - t \langle \ell^- | K | \ell^- \rangle) f(\lambda_\ell, \tilde{\lambda}_\ell, t).
\end{aligned} \tag{4.45}$$

In the kinematic region $K^2 > 0$, the delta function is non-vanishing when the integration over t is performed,

$$C_2 = \int \langle \ell d\ell \rangle [\ell d\ell] \frac{K^2}{\langle \ell^- | K | \ell^- \rangle^2} f\left(\lambda_\ell, \tilde{\lambda}_\ell, t = \frac{K^2}{\langle \ell^- | K | \ell^- \rangle}\right). \tag{4.46}$$

It is possible to split f into functions whose numerators depend only on λ_ℓ , whose integration gives rise to box integrals and three-mass triangle integrals, and remaining terms whose numerators depend on both λ_ℓ and $\tilde{\lambda}_\ell$. For the latter terms, the key idea is to rewrite the cut as a total derivative of the form,

$$C_2 = \int \langle \ell d\ell \rangle [d\ell \partial_\ell] g(\lambda_\ell, \tilde{\lambda}_\ell), \tag{4.47}$$

plus a set of residues. The total derivative integrates to zero. The residues arise from $1/\langle \ell a \rangle$ poles in $g(\lambda_\ell, \tilde{\lambda}_\ell)$. At these singularities, one obtains delta-function contributions [109] using,

$$[d\ell \partial_\ell] \frac{1}{\langle \ell a \rangle} = -2\pi \bar{\delta}(\langle \ell a \rangle), \tag{4.48}$$

where $\int \langle \ell d\ell \rangle \bar{\delta}(\langle \ell a \rangle) A(\lambda_\ell, \tilde{\lambda}_\ell) = -iA(\lambda_a, \tilde{\lambda}_a)$. This localization by delta functions relies on treating λ_ℓ and $\tilde{\lambda}_\ell$ as complex conjugates [93]. The delta functions allow us to replace the spinor integration variable λ_ℓ with spinors of the external momenta, since the delta-function condition in eq. (4.48) is satisfied whenever $\lambda_\ell \propto \lambda_a$ and $\tilde{\lambda}_\ell \propto \tilde{\lambda}_a$. (The constant of proportionality always drops out.)

In more complicated cases, where there are multiple poles in $\tilde{\lambda}_\ell$, one must first perform a partial-fraction decomposition or a Feynman parametrization in order to rewrite the integrand as a total derivative plus localized contributions. This procedure has also been extended to the cases of D -dimensional unitarity [58] and massive particles circulating in the loop [60].

5. On-Shell Recursion at One Loop

In this section, we discuss how to compute rational terms in one-loop amplitudes. We assume that the terms containing cuts have already been computed via four-dimensional unitarity, as described in the previous section. A number of analytic methods for determining the rational terms have been proposed in the literature. A recent proposal is to make use of D -dimensional unitarity [70,58,60], following the early work in refs. [46,71]. Another proposal relies on the observation that only a limited number of loop-momentum integrals can contribute to rational terms, making their evaluation simpler [40,41]. In this review, we focus on the on-shell recursive approach [52,53,54,55,56]. This approach is quite promising because it displays only mild growth in computational complexity as

the number of external legs increases. (In special cases, the pole structure of the rational coefficients in front of integral functions is well-enough constrained that they can be computed using this technique too, instead of using unitarity [110].)

At one loop as at tree level, on-shell recursion provides a systematic means of determining rational functions, using knowledge of their poles and residues. At loop level, however, there are a number of new issues that must be confronted.

The most obvious issue is the appearance of branch cuts in the shifted amplitude. We will find it helpful to distinguish between terms that contain such cuts and terms that do not. Let us break up a one-loop amplitude, shifted by a $[j, l]$ shift, as follows,

$$A_n^{1\text{-loop}}(z) = c_\Gamma \left[C_n(z) + R_n(z) \right]. \quad (5.1)$$

where $C_n(z)$ denotes the pure cut-containing terms, and $R_n(z)$ gives the rational terms. The rational parts R_n are defined by setting all logarithms, polylogarithms, and associated π^2 terms to zero,

$$R_n \equiv \frac{1}{c_\Gamma} A_n^{1\text{-loop}} \Big|_{\text{rat}} \equiv \frac{1}{c_\Gamma} A_n^{1\text{-loop}} \Big|_{\ln, \text{Li}, \pi^2 \rightarrow 0}. \quad (5.2)$$

We assume that the cut-containing terms C_n have already been computed.

As discussed in section 4.5, loop amplitudes contain spurious poles that cancel only between the cut-containing and rational contributions. Such spurious poles would complicate the on-shell recursion relations because they would require us to compute residues at poles corresponding to unphysical singularities. Such singularities are not singularities of the total amplitude at all. The simplest approach is to eliminate them completely. We can do this by adding in rational terms that manifestly cancel all spurious singularities, before applying Cauchy's theorem to the other rational terms. We gave examples of such 'cut completions', associated with the structure of two-mass triangle integrals, in section 4.5. These completions introduce functions $L_i(r)$ defined in eq. (4.42), which are nonsingular as $r \rightarrow 1$. More intricate spurious singularities can also arise. One can make their absence manifest using functions (based on higher-dimensional box and triangle integrals) introduced in ref. [111].

In general, we denote the cut completion by \widehat{C}_n ,

$$\widehat{C}_n(z) = C_n(z) + \widehat{C}R_n(z), \quad (5.3)$$

where $\widehat{C}R_n(z)$ are the rational functions added in order to cancel the unphysical spurious singularities in z . For a given shift we do not need to remove all spurious singularities, but only those that depend on z . Having added rational terms to the cuts, we must subtract them from the rational part of the amplitude. This procedure defines the 'remaining' rational terms,

$$\widehat{R}_n(z) = R_n(z) - \widehat{C}R_n(z). \quad (5.4)$$

Instead of the pure-cut plus pure-rational decomposition (5.1), we thus consider the completed-cut decomposition,

$$A_n^{1\text{-loop}}(z) = c_\Gamma \left[\widehat{C}_n(z) + \widehat{R}_n(z) \right], \quad (5.5)$$

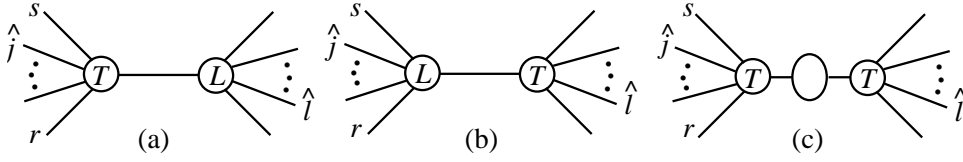


Fig. 12. Diagrammatic representation of recursive contributions at one loop with a $[j, l]$ shift. The labels ‘T’ and ‘L’ on the vertices indicate tree and loop vertices, respectively. The factorization-function contribution (c) does not appear for MHV amplitudes.

and analyze the properties of $\widehat{R}_n(z)$ in the complex plane. This decomposition is not unique; rational functions having no spurious singularities can be moved between \widehat{C}_n and \widehat{R}_n .

As a concrete example, consider the cut parts of the scalar-loop contribution to the five-point amplitude $A_5^{\text{scalar}}(1^-, 2^-, 3^+, 4^+, 5^+)$ given in eq. (4.43). The L_i functions defined in eq. (4.42) incorporate rational terms and automatically provide a satisfactory cut completion for this amplitude. The spurious poles located at $s_{23} - s_{51} = 0$ are manifestly absent from the cut parts. Hence they will also not appear in the remaining rational terms.

In general, the complete amplitude cannot have any unphysical poles. After we eliminate them from the completed-cut parts, they cannot appear in the remaining rational terms $\widehat{R}_n(z)$ either. We can then construct an on-shell recursion relation for $\widehat{R}_n(z)$, summing only over residues at physical poles [54,55]. The terms in the sum are in one-to-one correspondence with the factorization channels, just as at tree level. At one loop, though, there are typically more terms in each channel. For each intermediate state helicity, there are generically three contributions to one-loop factorization as $K_{r\dots s}^2 \rightarrow 0$, which are depicted in fig. 12,

$$A_n^{1\text{-loop}} \sim A_L^{\text{tree}} \frac{i}{K_{r\dots s}^2} A_R^{1\text{-loop}} + A_L^{1\text{-loop}} \frac{i}{K_{r\dots s}^2} A_R^{\text{tree}} + A_L^{\text{tree}} \frac{i \mathcal{F}^{1\text{-loop}}}{K_{r\dots s}^2} A_R^{\text{tree}}. \quad (5.6)$$

In the first two terms, one of the factorized amplitudes is a one-loop amplitude and the other is a tree amplitude. The last term naively corresponds to a one-loop correction to the propagator. However, massless theories contain infrared divergences from soft and collinear virtual momenta. These divergences do not commute with the factorization limit $K_{r\dots s}^2 \rightarrow 0$. For this reason, the ‘factorization function’ $\mathcal{F}^{1\text{-loop}}$ is more subtle in massless theories; it can contain ‘pole-crossing’ logarithms (logarithms of momentum invariants containing momenta from both sides of the pole) [112]. However, we are only interested in the rational terms. These terms do have a simple interpretation in terms of propagator corrections.

Following similar logic as at tree level, and dropping the pure-cut pieces in eq. (5.6), we obtain an on-shell recursion relation for the rational terms, corresponding to the diagrams in fig. 12,

$$\begin{aligned} R_n^D &\equiv - \sum_{\text{poles } \alpha} \text{Res}_{z=z_\alpha} \frac{R_n(z)}{z} \\ &= \sum_{r,s,h} \left\{ R_L(z=z_{rs}) \frac{i}{K_{r\dots s}^2} A_R^{\text{tree}}(z=z_{rs}) + A_L^{\text{tree}}(z=z_{rs}) \frac{i}{K_{r\dots s}^2} R_R(z=z_{rs}) \right\} \end{aligned}$$

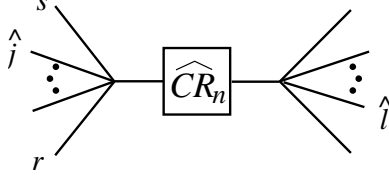


Fig. 13. A generic overlap contribution with a $[j, l]$ shift. The diagram indicates the channel where the residue is to be extracted.

$$+ A_L^{\text{tree}}(z = z_{rs}) \frac{i\mathcal{F}(K_{r\dots s})}{K_{r\dots s}^2} A_R^{\text{tree}}(z = z_{rs}) \Bigg\}. \quad (5.7)$$

The ‘vertices’ R_L and R_R in this recursion relation are the pure rational parts (according to the definition (5.2) of the lower-point one-loop amplitudes appearing on the left and right sides of eq. (5.6). The factorization function \mathcal{F} may be found in ref. [55]. It only contributes in multi-particle channels, and only if the tree amplitude contains a pole in that channel. The superscript D on R_n^D indicates that this set of (recursive) diagrammatic contributions to the remaining rational terms \hat{R}_n is not the whole answer.

We have included some of the rational terms \widehat{CR}_n in the completed cuts \hat{C}_n in shifting from eq. (5.1) to (5.5). Therefore we need to correct eq. (5.7) for any residues that $\widehat{CR}_n(z)$ may have at the physical poles. We know \widehat{CR}_n explicitly, so it is simple to compute the correction or ‘overlap’ terms O_n by performing the shift (2.20) and extracting the residues of $\widehat{CR}_n(z)$ at each physical pole,

$$O_n \equiv \sum_{\text{poles } \alpha} \text{Res}_{z=z_\alpha} \frac{\widehat{CR}_n(z)}{z}. \quad (5.8)$$

These overlap contributions may be assigned a diagrammatic interpretation, as depicted in fig. 13. Each diagram corresponds to a different physical factorization channel. Although the definition of the completed-cut terms \hat{C}_n is not unique, the ambiguity cancels in the sum of $\hat{C}_n(0)$ and the overlap terms O_n .

We are not yet done, because we have not discussed the behavior of the shifted one-loop amplitude at large z . The straightforward application of Cauchy’s theorem underlying our computation requires that the shift of the remaining rational parts $\hat{R}_n(z)$ fall off as $z \rightarrow \infty$. At tree level, as discussed in section 3, one can prove that $A_n^{1\text{-loop}}(z)$ vanishes as $z \rightarrow \infty$ for various classes of shifts. At one loop there are no such theorems, and we are sometimes forced to use shifts for which $A_n^{1\text{-loop}}(z)$ does not vanish. Let us denote by $\text{Inf } A_n^{1\text{-loop}}$ a function which, when shifted, matches the behavior of $A_n^{1\text{-loop}}(z)$ as $z \rightarrow \infty$, that is $A_n^{1\text{-loop}}(z) - \text{Inf } A_n^{1\text{-loop}}(z) \rightarrow 0$ as $z \rightarrow \infty$. (This function is rational in the existing examples.) A practical approach for determining $\text{Inf } A_n^{1\text{-loop}}$ is by using an auxiliary on-shell recursion relation [55]. The completed-cut terms $\hat{C}_n(z)$ may also be nonvanishing at large z ; we define an analogous function $\text{Inf } \hat{C}_n$ which matches their large z behavior. Neither $\text{Inf } A_n^{1\text{-loop}}$ nor $\text{Inf } \hat{C}_n$ contains poles at finite z , so they do not affect eqs. (5.7) and (5.8).

Putting together all the different pieces, the full one-loop amplitude is [55],

$$A_n^{1\text{-loop}}(0) = \text{Inf } A_n^{1\text{-loop}} + c_\Gamma \left[\hat{C}_n(0) - \text{Inf } \hat{C}_n + R_n^D + O_n \right]. \quad (5.9)$$

Equivalently, the terms to be added to the completed-cut terms \widehat{C}_n are,

$$\widehat{R}_n = \frac{1}{c_T} \text{Inf } A_n^{1\text{-loop}} - \text{Inf } \widehat{C}_n + R_n^D + O_n. \quad (5.10)$$

The role of $\text{Inf } A_n^{1\text{-loop}}$ and $(-\text{Inf } \widehat{C}_n)$ is to ensure the proper large- z behavior under the shift. The overlap terms O_n remove double-counting of residues at physical poles between the completed-cut terms $\widehat{C}_n(0)$ and the recursive diagrams R_n^D .

One subtlety connected with the use of complex momenta is the appearance of physical poles at finite values of z whose residues are not known *a priori*. The factorization properties of amplitudes with real external momenta are well studied at tree and loop level [78,44,112,113,67]. In multi-particle factorization channels, this information is sufficient to evaluate the residues at the complex poles corresponding to the recursive diagrams in eq. (5.7). However, factorization in two-particle channels, such as in eq. (2.24), is more subtle in complex kinematics than in real kinematics.

The additional complexity in two-particle channels is due to the fact that, in a real collinear limit, $k_i \parallel k_j$, the spinor products $\langle i j \rangle$ and $[i j]$ vanish at the same rate, whereas one of the two remains nonzero in complex on-shell three-point kinematics. In a particular collinear limit where gluons i and j have positive helicity, and the intermediate gluon with momentum K_{ij} has negative helicity, there is a potential violation of helicity conservation by 3 units. Associated with this is a collinear behavior

$$A(\dots, i^+, j^+, \dots) \sim \frac{[i j]}{\langle i j \rangle^2}. \quad (5.11)$$

Such behavior is absent at tree level, because as noted in eq. (2.19), $A_3^{\text{tree}}(1^+, 2^+, 3^+)$ vanishes. The typical tree-level behavior in a collinear limit is $A \sim 1/\langle i j \rangle$ or $A \sim 1/[i j]$. At one loop, the behavior (5.11) does arise. For real kinematics, the behavior in eq. (5.11) is equally singular in magnitude, $|A| \sim 1/\sqrt{s_{ij}}$. With complex momenta, however, one can approach a kinematic point at which $\langle i j \rangle$ vanishes but $[i j]$ does not; the more singular behavior (5.11) then leads to double poles in the z plane. The residues in such channels are not yet fully understood, and may not even be universal, because they peer deeper into the Taylor expansion around the pole.

One can also find examples of channels in which loop amplitudes contain ‘unreal poles’ $[i j] / \langle i j \rangle$ which can be singular for complex momenta but are finite for real momenta [53]. At tree level this phenomenon also does not occur. As the residues at unreal poles are not yet fully understood either, the best strategy is to choose shifts that avoid channels with unknown factorization properties. For n -gluon amplitudes the problematic channels always have precisely two identical-helicity gluons on one side of the factorization, as in eq. (5.11). A general strategy for avoiding such channels has been given in ref. [55].

5.1. One-loop five-point example

We illustrate the on-shell recursive approach to determining loop amplitudes by re-computing the rational part of a one-loop five-gluon QCD amplitude first computed in ref. [114].

Consider the amplitude $A_5^{\text{scalar}}(1^-, 2^-, 3^+, 4^+, 5^+)$ for five external gluons, with a colored scalar circulating in the loop. We begin with the cut-containing parts of this ampli-

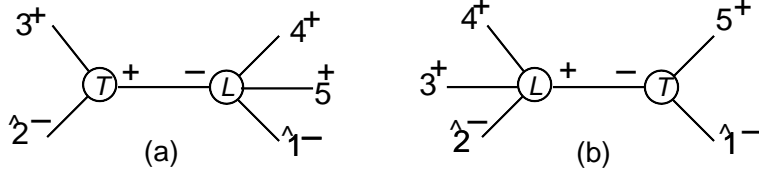


Fig. 14. The recursive diagrams for computing the rational parts of $A_5^{\text{scalar}}(1^-, 2^-, 3^+, 4^+, 5^+)$ with the $[1, 2]$ shift given in eq. (5.14). ‘T’ signifies a tree vertex and ‘L’ a loop vertex.

tude. They are given in eq. (4.43). For convenience, in defining the completed-cut terms \widehat{C}_5 we add in a rational term proportional to the tree amplitude. (As explained in the last section, we are free to add any rational terms that do not introduce new spurious singularities in z .) We use,

$$\widehat{C}_5 = \frac{1}{c_{\Gamma}} A_5^{\text{scalar}}(1^-, 2^-, 3^+, 4^+, 5^+) \Big|_{\text{cut-containing}} + \frac{8}{9} A_5^{\text{tree}}(1^-, 2^-, 3^+, 4^+, 5^+), \quad (5.12)$$

where the tree amplitude is given in eq. (2.16), with $j = 1$, $k = 2$ and $n = 5$. Taking the rational part of this expression gives

$$\begin{aligned} \widehat{CR}_5 = & i \left(\frac{1}{3\epsilon} + \frac{8}{9} \right) \frac{\langle 12 \rangle^4}{\langle 12 \rangle \langle 23 \rangle \langle 34 \rangle \langle 45 \rangle \langle 51 \rangle} - \frac{i}{6} \frac{s_{51} + s_{23}}{s_{23}s_{51}(s_{51} - s_{23})^2} \\ & \times \frac{[34] \langle 41 \rangle \langle 24 \rangle [45] \left(\langle 23 \rangle [34] \langle 41 \rangle + \langle 24 \rangle [45] \langle 51 \rangle \right)}{\langle 34 \rangle \langle 45 \rangle}, \end{aligned} \quad (5.13)$$

which is needed to determine the overlap terms.

We construct the rational parts using a $[1, 2]$ shift,

$$\tilde{\lambda}_1 \rightarrow \tilde{\lambda}_1 - z\tilde{\lambda}_2, \quad \lambda_2 \rightarrow \lambda_2 + z\lambda_1. \quad (5.14)$$

We will assume that the shifted amplitude vanishes at large z , so that $\text{Inf } A_5 = 0$. We can verify the validity of this assumption at the end of the calculation. It is not difficult to check that the rational part of the cut term \widehat{CR}_5 , given in eq. (5.13), vanishes at large z ; thus $\text{Inf } \widehat{C}_5 = 0$ as well in this example.

With the $[1, 2]$ shift, all diagrams (including loop diagrams) with a $(--+)$ -type three-vertex containing leg 2 vanish. Similarly, all diagrams with a $(-++)$ -type three-vertex containing leg 1 also vanish. One-loop three-vertices for which the external gluons have opposite helicity vanish as well. Some of these vanishings are related to those of tree-level three-vertices with ‘wrong’ kinematic solutions, as explained in ref. [55].

We have just two nonvanishing recursive diagrams. Diagram (a) in fig. 14 is given by

$$D_5^{(a)} = A_3^{\text{tree}}(\hat{2}^-, 3^+, -\hat{K}_{23}^+) \frac{i}{s_{23}} R_4(\hat{1}^-, \hat{K}_{23}^-, 4^+, 5^+). \quad (5.15)$$

The required three-point tree amplitude is given in eq. (2.18). The four-vertex is easily constructed from the known four-point amplitude [102],

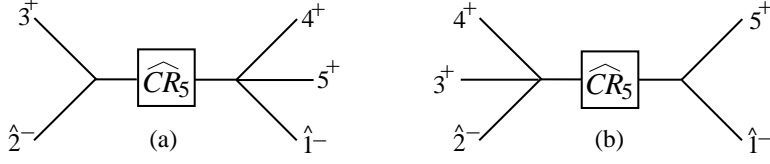


Fig. 15. The five-point overlap diagrams using the $[1, 2]$ shift given in eq. (5.14).

$$A_4^{\text{scalar}}(1^-, 2^-, 3^+, 4^+) = c_\Gamma A_4^{\text{tree}}(1^-, 2^-, 3^+, 4^+) \left(\frac{1}{3\epsilon} - \frac{1}{3} \ln \left(\frac{-s_{23}}{\mu^2} \right) + \frac{8}{9} \right). \quad (5.16)$$

Following eq. (5.2) and setting the logarithm to zero gives us the four-vertex,

$$R_4(1^-, 2^-, 3^+, 4^+) = \left(\frac{1}{3\epsilon} + \frac{8}{9} \right) A_4^{\text{tree}}(1^-, 2^-, 3^+, 4^+). \quad (5.17)$$

Because this vertex is proportional to the four-point tree amplitude, the evaluation of this diagram is identical to the (unique) recursive diagram for the five-point tree amplitude with the same helicities and shift. The result is

$$D_5^{(a)} = i \left(\frac{1}{3\epsilon} + \frac{8}{9} \right) \frac{\langle 12 \rangle^4}{\langle 12 \rangle \langle 23 \rangle \langle 34 \rangle \langle 45 \rangle \langle 51 \rangle}. \quad (5.18)$$

The second diagram is,

$$D_5^{(b)} = A_3^{\text{tree}}(5^+, \hat{1}^-, -\hat{K}_{51}^-) \times \frac{i}{s_{51}} \times R_4(\hat{2}^-, 3^+, 4^+, \hat{K}_{51}^+). \quad (5.19)$$

Again the one-loop four-vertex comes directly from the known four-point amplitude [102]. For this helicity configuration, the amplitude is purely rational so we have

$$R_4(1^-, 2^+, 3^+, 4^+) = \frac{1}{c_\Gamma} A_4^{\text{scalar}}(1^-, 2^+, 3^+, 4^+) = \frac{i}{3} \frac{\langle 24 \rangle [24]^3}{[12] \langle 23 \rangle \langle 34 \rangle [41]}. \quad (5.20)$$

The diagram evaluates to,

$$\begin{aligned} D_5^{(b)} &= -\frac{i}{3} \frac{\langle \hat{1}(-\hat{K}_{51}) \rangle^3}{\langle 5\hat{1} \rangle \langle (-\hat{K}_{51})5 \rangle} \frac{1}{s_{51}} \frac{\langle 3\hat{K}_{51} \rangle [3\hat{K}_{51}]^3}{[\hat{2}3] \langle 34 \rangle \langle 4\hat{K}_{51} \rangle [\hat{K}_{51}\hat{2}]} \\ &= \frac{i}{3} \frac{\langle 1^- | 5 | 2^- \rangle^3}{\langle 51 \rangle \langle 5^- | 1 | 2^- \rangle} \frac{1}{\langle 51 \rangle [15] \langle 1^- | 5 | 2^- \rangle^2} \frac{\langle 3^- | 4 | 2^- \rangle \langle 1^- | 5 | 3^- \rangle^3}{[23] \langle 34 \rangle \langle 4^- | 3 | 2^- \rangle \langle 1^- | 5 | 2^- \rangle} \\ &= -\frac{i}{3} \frac{[24][35]^3}{\langle 34 \rangle [12][15][23]^2}. \end{aligned} \quad (5.21)$$

The overlap contributions from eq. (5.8) are depicted in fig. 15. The rational parts of the completed-cut terms, \widehat{CR}_5 , are given in eq. (5.13). Applying the shift (5.14) to \widehat{CR}_5 , we obtain,

$$\widehat{CR}_5(z) = i \left(\frac{1}{3\epsilon} + \frac{8}{9} \right) \frac{\langle 12 \rangle^4}{\langle 12 \rangle (\langle 23 \rangle + z \langle 13 \rangle) \langle 34 \rangle \langle 45 \rangle \langle 51 \rangle}$$

$$\begin{aligned}
& -\frac{i}{6} \frac{[34] \langle 41 \rangle (\langle 24 \rangle + z \langle 14 \rangle) [45]}{\langle 34 \rangle \langle 45 \rangle} \\
& \times \frac{(\langle 23 \rangle + z \langle 13 \rangle) [34] \langle 41 \rangle + (\langle 24 \rangle + z \langle 14 \rangle) [45] \langle 51 \rangle}{(\langle 23 \rangle + z \langle 13 \rangle) [32] \langle 15 \rangle} \\
& \times \frac{s_{51} + s_{23} - z \langle 1^- | 5 | 2^- \rangle + z \langle 1^- | 3 | 2^- \rangle}{([51] - z [52])(s_{51} - s_{23} - z \langle 1^- | (5+3) | 2^- \rangle)^2}.
\end{aligned} \tag{5.22}$$

The residues of $\widehat{CR}_5(z)/z$ have to be evaluated at the following values of z ,

$$z^{(a)} = -\frac{\langle 23 \rangle}{\langle 13 \rangle}, \quad z^{(b)} = \frac{[15]}{[25]}, \tag{5.23}$$

corresponding to the two overlap diagrams in fig. 15. The first residue is

$$O_5^{(a)} = -i \left(\frac{1}{3\epsilon} + \frac{8}{9} \right) \frac{\langle 12 \rangle^4}{\langle 12 \rangle \langle 23 \rangle \langle 34 \rangle \langle 45 \rangle \langle 51 \rangle} - \frac{i}{6} \frac{\langle 12 \rangle^2 \langle 14 \rangle [34]}{\langle 15 \rangle \langle 23 \rangle \langle 34 \rangle \langle 45 \rangle [23]}. \tag{5.24}$$

With our choice of cut completion (5.12), the singular term and associated rational terms cancel between the recursive and overlap contributions in eqs. (5.18) and (5.24). The second overlap diagram, shown in fig. 15(b), gives

$$O_5^{(b)} = \frac{i}{6} \frac{\langle 14 \rangle [34] [35] (\langle 14 \rangle [34] - \langle 15 \rangle [35])}{\langle 15 \rangle \langle 34 \rangle \langle 45 \rangle [15] [23]^2}. \tag{5.25}$$

Summing over the contributions to eq. (5.10), with $\text{Inf } A_5 = \text{Inf } \widehat{C}_5 = 0$, we obtain,

$$\begin{aligned}
\widehat{R}_5 &= D_5^{(a)} + D_5^{(b)} + O_5^{(a)} + O_5^{(b)} \\
&= \frac{i}{6} \left(-\frac{2 [24] [35]^3}{\langle 34 \rangle [12] [15] [23]^2} - \frac{\langle 12 \rangle^2 \langle 14 \rangle [34]}{\langle 15 \rangle \langle 23 \rangle \langle 34 \rangle \langle 45 \rangle [23]} \right. \\
&\quad \left. + \frac{\langle 14 \rangle^2 [34]^2 [35]}{\langle 15 \rangle \langle 34 \rangle \langle 45 \rangle [15] [23]^2} - \frac{\langle 14 \rangle [34] [35]^2}{\langle 34 \rangle \langle 45 \rangle [15] [23]^2} \right).
\end{aligned} \tag{5.26}$$

The full amplitude is the sum of \widehat{R}_5 and the completed-cut terms \widehat{C}_5 from eq. (5.12). The sum agrees with the result of ref. [114].

This procedure has been applied to generate a variety of amplitudes, including the n -gluon amplitudes with two negative-helicity gluons, and the rest of positive helicity [54,55], which are the one-loop analogs of the MHV tree amplitudes in eq. (2.16).

6. Conclusions and Outlook

Next-to-leading order computations of QCD processes will play an important role in understanding and interpreting results from the forthcoming Large Hadron Collider. The current state of the art, at parton level, is for the production of three final-state objects, requiring one-loop five-point amplitudes. New approaches proposed for one-loop amplitudes with six or more external legs fall into three general categories: purely numerical [43,29], improved traditional (including semi-numerical) [31,32,33,34,35,36,37,38,39,40,41,42], ■

and on-shell analytic methods [44,45,46,47,48,49,50,51,52,53,54,55,56,57,58,59,60]. The status of state-of-the-art calculations with these methods has been summarized in the Introduction.

This review has focused primarily on on-shell methods for loop calculations. An early version of on-shell methods has been used to compute the one-loop amplitudes for $e^+e^- \rightarrow Z \rightarrow 4$ partons and (by crossing) for $pp \rightarrow W, Z + 2$ jets [64]. The latter have been implemented in the MCFM program [25]. More recently, on-shell methods have been used to obtain a variety of one-loop QCD amplitudes, both particular sequences of helicity amplitudes containing an arbitrary number of external gluons, as well as four of six helicity configurations for six gluons [48,50,51,57,55,56]. These computations make use of recent advances in the evaluation of coefficients of loop integrals [49,51,57] within the framework of the unitarity method [44,45], as well as loop-level on-shell recursion for the rational terms [52,53,54,55], based on the BCFW [8,9] tree-level on-shell recursion. (The cut-containing parts of the remaining two helicity configurations in the six-gluon amplitude were also determined in this way [51,57], while the rational parts were computed in ref. [40].) The analytical results agree numerically (where they have been compared) with the semi-numerical results of ref. [39]. Other loop-level developments include various improvements [70,58] to the D -dimensional variant of the unitarity method [46].

The challenge now is to provide complete one-loop QCD results for more complex processes, for all possible partonic subprocesses and for all possible helicity configurations. Especially important phenomenologically are processes including electroweak vector bosons, heavy quarks and Higgs bosons in the final state. The six-gluon computations have outlined effective analytical techniques, but more automation will be required to handle all the cases needed for complete NLO predictions.

On-shell methods offer the promise of a relatively modest growth in complexity as the number of external legs increases, due to the recursive structure. The unitarity method builds one-loop amplitudes directly from known on-shell tree amplitudes. In its four-dimensional variant, it provides an efficient means for generating the coefficients of the basis integrals, while the D -dimensional variant can be used to compute complete amplitudes. Loop-level on-shell recursion can be used to determine rational terms, using as input the cut-containing terms and lower-point rational terms. Together they yield complete amplitudes.

The one-loop multi-parton matrix elements are most often the only missing ingredient needed to construct a numerical program for NLO differential cross sections. Writing such programs is a non-trivial task, but general formalisms are available for doing so [17,18,19,20]. The implementation of the matrix elements in these programs raises a number of practical issues, including the speed of numerical evaluation and numerical stability. One would need operational NLO programs to study these issues more carefully, but early indications are promising for the forms of the results found using on-shell methods. For example, speed comparisons between the on-shell and semi-numerical approach for six-gluon amplitudes [39,56] indicate a rather significant speed advantage for the former method.

Studies of numerical stability, due to round-off error near spurious singularities, have not been performed for amplitudes recently constructed by on-shell methods. However, experience with the processes $pp \rightarrow W, Z + 2$ jets [115] and $e^+e^- \rightarrow 4$ jets [116] indicates that these methods produce analytic expressions for amplitudes [64] with sufficiently mild singular behavior that numerical stability is not an issue. As explained in

ref. [111], the widths of numerically unstable regions depend heavily on the powers to which potentially-singular denominator factors are raised. Singularities that cancel within the functions used in the cut completion, such as the L_i functions, can easily be patched, using Taylor expansions, in their numerical implementation. The remaining spurious singularities appearing in the matrix elements do not cause any difficulties [115,116]. This evidence suggests that NLO programs using higher-point amplitudes computed from on-shell methods should also be free of significant round-off instabilities. Of course, this suggestion will need to be confirmed with detailed studies. Beyond the application to parton-level physics programs, it will be important to interface new one-loop matrix elements to the new generation of parton showering programs [15,16].

The techniques described in this review can be applied directly to processes involving quarks and external vector bosons. Such processes are of crucial importance for understanding backgrounds to new physics such as supersymmetry or other extensions of the Standard Model. Other processes of interest containing massive particles inside the loop, such as top production, will require further development. Recent progress on applying D -dimensional unitarity [46,70,58] to massive particles in the loops may be found in ref. [60].

The large number of subprocesses needed for new applications to collider phenomenology makes it highly desirable to have an automated program for evaluating the amplitudes. The on-shell methods we have discussed in this review are systematic and thus should lend themselves to automation, although much more work is required to substantiate this assertion.

Besides the remaining practical issues there are a number of open theoretical issues. The analytic properties of loop amplitudes with complex momenta are not as well understood as one might like. In particular, we have an incomplete understanding of the ‘unreal’ poles encountered in on-shell recursion at the loop level. The best strategy for dealing with these poles at present is to set up recursion relations that avoid them. A first-principles understanding of properties of one-loop scattering amplitudes, under factorization with complex momenta, and at large values of the complex shift parameter, would be very helpful. One possible avenue for investigating these properties is the link between tree-level on-shell recursion relations and Feynman rules [117] in a variant of light-cone gauge called space-cone gauge [118]. Unitarity in D dimensions [46] may also assist in this formal understanding.

We anticipate that the on-shell methods described in this review will, with further development, be widely applicable to the higher-multiplicity amplitudes required for next-to-leading order computations of phenomenological interest at the Large Hadron Collider.

Acknowledgments

We thank Carola Berger and Darren Forde for collaboration on topics presented in this review. We also thank Bo Feng for helpful discussions. The figures were generated using Jaxodraw [119], based on Axodraw [120].

References

- [1] T. Stelzer and W. F. Long, Comput. Phys. Commun. **81**, 357 (1994) [hep-ph/9401258].
- [2] A. Pukhov *et al.*, hep-ph/9908288.
- [3] F. Krauss, R. Kuhn and G. Soff, JHEP **0202**, 044 (2002) [hep-ph/0109036].
- [4] M. L. Mangano, M. Moretti, F. Piccinini, R. Pittau and A. D. Polosa, JHEP **0307**, 001 (2003) [hep-ph/0206293].
- [5] A. Kanaki and C. G. Papadopoulos, Comput. Phys. Commun. **132**, 306 (2000) [hep-ph/0002082].
- [6] F. A. Berends and W. T. Giele, Nucl. Phys. B **306**, 759 (1988).
- [7] D. A. Kosower, Nucl. Phys. B **335**, 23 (1990);
F. Caravaglios and M. Moretti, Phys. Lett. B **358**, 332 (1995) [hep-ph/9507237];
P. Draggiotis, R. H. P. Kleiss and C. G. Papadopoulos, Phys. Lett. B **439**, 157 (1998) [hep-ph/9807207];
F. Caravaglios, M. L. Mangano, M. Moretti and R. Pittau, Nucl. Phys. B **539**, 215 (1999) [hep-ph/9807570].
- [8] R. Britto, F. Cachazo and B. Feng, Nucl. Phys. B **715**, 499 (2005) [hep-th/0412308].
- [9] R. Britto, F. Cachazo, B. Feng and E. Witten, Phys. Rev. Lett. **94**, 181602 (2005) [hep-th/0501052].
- [10] F. A. Berends, W. T. Giele and H. Kuijf, Nucl. Phys. B **321**, 39 (1989).
- [11] H. U. Bengtsson and T. Sjöstrand, Comput. Phys. Commun. **46**, 43 (1987);
T. Sjöstrand, P. Eden, C. Friberg, L. Lönnblad, G. Miu, S. Mrenna and E. Norrbin, Comput. Phys. Commun. **135**, 238 (2001) [hep-ph/0010017].
- [12] G. Marchesini and B. R. Webber, Cavendish-HEP-87/9;
G. Marchesini, B. R. Webber, G. Abbiendi, I. G. Knowles, M. H. Seymour and L. Stanco, Comput. Phys. Commun. **67**, 465 (1992);
G. Corcella *et al.*, hep-ph/0210213.
- [13] S. Catani, F. Krauss, R. Kuhn and B. R. Webber, JHEP **0111**, 063 (2001) [hep-ph/0109231];
S. Mrenna and P. Richardson, JHEP **0405**, 040 (2004) [hep-ph/0312274];
M. Mangano, presented at the Fermilab ME/MC Tuning Workshop, October 4, 2004;
S. Höche, F. Krauss, N. Lavesson, L. Lönnblad, M. Mangano, A. Schälicke and S. Schumann, hep-ph/0602031;
M. L. Mangano, M. Moretti, F. Piccinini and M. Treccani, JHEP **0701**, 013 (2007) [hep-ph/0611129].
- [14] S. Catani, D. de Florian and M. Grazzini, JHEP **0105**, 025 (2001) [hep-ph/0102227];
R. V. Harlander and W. B. Kilgore, Phys. Rev. Lett. **88**, 201801 (2002) [hep-ph/0201206];
C. Anastasiou and K. Melnikov, Nucl. Phys. B **646**, 220 (2002) [hep-ph/0207004];
V. Ravindran, J. Smith and W. L. van Neerven, Nucl. Phys. B **665**, 325 (2003) [hep-ph/0302135].
- [15] S. Frixione and B. R. Webber, JHEP **0206**, 029 (2002) [hep-ph/0204244];
S. Frixione, P. Nason and B. R. Webber, JHEP **0308**, 007 (2003) [hep-ph/0305252].
- [16] P. Nason, JHEP **0411**, 040 (2004) [hep-ph/0409146];
Z. Nagy and D. E. Soper, JHEP **0510**, 024 (2005) [hep-ph/0503053];
M. Krämer, S. Mrenna and D. E. Soper, Phys. Rev. D **73**, 014022 (2006) [hep-ph/0509127];
P. Nason and G. Ridolfi, JHEP **0608**, 077 (2006) [hep-ph/0606275];
O. Latunde-Dada, S. Gieseke and B. Webber, JHEP **0702**, 051 (2007) [hep-ph/0612281].
- [17] Z. Kunszt and D. E. Soper, Phys. Rev. D **46**, 192 (1992);
S. Frixione, Z. Kunszt and A. Signer, Nucl. Phys. B **467**, 399 (1996) [hep-ph/9512328].
- [18] W. T. Giele and E. W. N. Glover, Phys. Rev. D **46**, 1980 (1992);
W. T. Giele, E. W. N. Glover and D. A. Kosower, Nucl. Phys. B **403**, 633 (1993) [hep-ph/9302225].
- [19] S. Catani and M. H. Seymour, Phys. Lett. B **378**, 287 (1996) [hep-ph/9602277]; Nucl. Phys. B **485**, 291 (1997) [Erratum-ibid. B **510**, 503 (1998)] [hep-ph/9605323].
- [20] S. Catani, S. Dittmaier, M. H. Seymour and Z. Trócsányi, Nucl. Phys. B **627**, 189 (2002) [hep-ph/0201036].
- [21] D. A. Kosower, Phys. Rev. D **57**, 5410 (1998) [hep-ph/9710213];
J. M. Campbell, M. A. Cullen and E. W. N. Glover, Eur. Phys. J. C **9**, 245 (1999) [hep-ph/9809429].
- [22] A. Gehrmann-De Ridder, T. Gehrmann and E. W. N. Glover, JHEP **0509**, 056 (2005) [hep-ph/0505111].

- [23] W. Beenakker, S. Dittmaier, M. Krämer, B. Plümper, M. Spira and P. M. Zerwas, Phys. Rev. Lett. **87**, 201805 (2001) [hep-ph/0107081]; Nucl. Phys. B **653**, 151 (2003) [hep-ph/0211352]; S. Dawson, L. H. Orr, L. Reina and D. Wackeroth, Phys. Rev. D **67**, 071503 (2003) [hep-ph/0211438]; S. Dawson, C. Jackson, L. H. Orr, L. Reina and D. Wackeroth, Phys. Rev. D **68**, 034022 (2003) [hep-ph/0305087].
- [24] W. B. Kilgore and W. T. Giele, Phys. Rev. D **55**, 7183 (1997) [hep-ph/9610433]. Z. Nagy, Phys. Rev. Lett. **88**, 122003 (2002) [hep-ph/0110315]; Phys. Rev. D **68**, 094002 (2003) [hep-ph/0307268].
- [25] J. Campbell and R. K. Ellis, Phys. Rev. D **65**, 113007 (2002) [hep-ph/0202176]; J. Campbell, R. K. Ellis and D. L. Rainwater, Phys. Rev. D **68**, 094021 (2003) [hep-ph/0308195].
- [26] S. Dawson, C. B. Jackson, L. Reina and D. Wackeroth, Mod. Phys. Lett. A **21**, 89 (2006) [hep-ph/0508293]; F. Febres Cordero, L. Reina and D. Wackeroth, Phys. Rev. D **74**, 034007 (2006) [hep-ph/0606102].
- [27] J. M. Campbell, R. K. Ellis and G. Zanderighi, JHEP **0610**, 028 (2006) [hep-ph/0608194].
- [28] A. Brandenburg, S. Dittmaier, P. Uwer and S. Weinzierl, Nucl. Phys. Proc. Suppl. **135**, 71 (2004) [hep-ph/0408137]; S. Dittmaier, P. Uwer and S. Weinzierl, hep-ph/0703120.
- [29] A. Lazopoulos, K. Melnikov and F. Petriello, hep-ph/0703273.
- [30] A. I. Davydchev, Phys. Lett. B **263**, 107 (1991).
- [31] A. Ferroglia, M. Passera, G. Passarino and S. Uccirati, Nucl. Phys. B **650**, 162 (2003) [hep-ph/0209219].
- [32] Y. Kurihara *et al.*, Nucl. Phys. B **654**, 301 (2003) [hep-ph/0212216]; Nucl. Phys. Proc. Suppl. **157**, 231 (2006).
- [33] A. Denner and S. Dittmaier, Nucl. Phys. B **658**, 175 (2003) [hep-ph/0212259]; Nucl. Phys. B **734**, 62 (2006) [hep-ph/0509141].
- [34] W. T. Giele and E. W. N. Glover, JHEP **0404**, 029 (2004) [hep-ph/0402152].
- [35] F. del Aguila and R. Pittau, JHEP **0407**, 017 (2004) [hep-ph/0404120].
- [36] R. K. Ellis, W. T. Giele and G. Zanderighi, Phys. Rev. D **72**, 054018 (2005) [Erratum-ibid. D **74**, 079902 (2006)] [hep-ph/0506196].
- [37] T. Binoth, J. P. Guillet, G. Heinrich, E. Pilon and C. Schubert, JHEP **0510**, 015 (2005) [hep-ph/0504267].
- [38] R. K. Ellis, W. T. Giele and G. Zanderighi, Phys. Rev. D **73**, 014027 (2006) [hep-ph/0508308].
- [39] R. K. Ellis, W. T. Giele and G. Zanderighi, JHEP **0605**, 027 (2006) [hep-ph/0602185].
- [40] Z. Xiao, G. Yang and C. J. Zhu, Nucl. Phys. B **758**, 53 (2006) [hep-ph/0607017].
- [41] T. Binoth, J. P. Guillet and G. Heinrich, JHEP **0702**, 013 (2007) [hep-ph/0609054].
- [42] G. Ossola, C. G. Papadopoulos and R. Pittau, Nucl. Phys. B **763**, 147 (2007) [hep-ph/0609007].
- [43] M. Krämer and D. E. Soper, Phys. Rev. D **66**, 054017 (2002) [hep-ph/0204113]; Z. Nagy and D. E. Soper, JHEP **0309**, 055 (2003) [hep-ph/0308127].
- [44] Z. Bern, L. J. Dixon, D. C. Dunbar and D. A. Kosower, Nucl. Phys. B **425**, 217 (1994) [hep-ph/9403226].
- [45] Z. Bern, L. J. Dixon, D. C. Dunbar and D. A. Kosower, Nucl. Phys. B **435**, 59 (1995) [hep-ph/9409265].
- [46] Z. Bern and A. G. Morgan, Nucl. Phys. B **467**, 479 (1996) [hep-ph/9511336]; Z. Bern, L. J. Dixon, D. C. Dunbar and D. A. Kosower, Phys. Lett. B **394**, 105 (1997) [hep-th/9611127].
- [47] Z. Bern, L. J. Dixon and D. A. Kosower, Nucl. Phys. Proc. Suppl. **51C**, 243 (1996) [hep-ph/9606378]; JHEP **0001**, 027 (2000) [hep-ph/0001001]; Z. Bern, A. De Freitas and L. J. Dixon, JHEP **0203**, 018 (2002) [hep-ph/0201161].
- [48] S. J. Bidder, N. E. J. Bjerrum-Bohr, L. J. Dixon and D. C. Dunbar, Phys. Lett. B **606**, 189 (2005) [hep-th/0410296].
- [49] R. Britto, F. Cachazo and B. Feng, Nucl. Phys. B **725**, 275 (2005) [hep-th/0412103].
- [50] S. J. Bidder, N. E. J. Bjerrum-Bohr, D. C. Dunbar and W. B. Perkins, Phys. Lett. B **612**, 75 (2005) [hep-th/0502028].
- [51] R. Britto, E. Buchbinder, F. Cachazo and B. Feng, Phys. Rev. D **72**, 065012 (2005) [hep-ph/0503132].
- [52] Z. Bern, L. J. Dixon and D. A. Kosower, Phys. Rev. D **71**, 105013 (2005) [hep-th/0501240].
- [53] Z. Bern, L. J. Dixon and D. A. Kosower, Phys. Rev. D **72**, 125003 (2005) [hep-ph/0505055].
- [54] Z. Bern, L. J. Dixon and D. A. Kosower, Phys. Rev. D **73**, 065013 (2006) [hep-ph/0507005]; D. Forde and D. A. Kosower, Phys. Rev. D **73**, 061701 (2006) [hep-ph/0509358].

- [55] C. F. Berger, Z. Bern, L. J. Dixon, D. Forde and D. A. Kosower, Phys. Rev. D **74**, 036009 (2006) [hep-ph/0604195].
- [56] C. F. Berger, Z. Bern, L. J. Dixon, D. Forde and D. A. Kosower, Phys. Rev. D **75**, 016006 (2007) [hep-ph/0607014].
- [57] R. Britto, B. Feng and P. Mastrolia, Phys. Rev. D **73**, 105004 (2006) [hep-ph/0602178].
- [58] C. Anastasiou, R. Britto, B. Feng, Z. Kunszt and P. Mastrolia, Phys. Lett. B **645**, 213 (2007) [hep-ph/0609191]; JHEP **0703**, 111 (2007) [hep-ph/0612277].
- [59] P. Mastrolia, Phys. Lett. B **644**, 272 (2007) [hep-th/0611091].
- [60] R. Britto and B. Feng, hep-ph/0612089.
- [61] Z. Nagy and D. E. Soper, Phys. Rev. D **74**, 093006 (2006) [hep-ph/0610028].
- [62] T. Binoth, T. Gehrmann, G. Heinrich and P. Mastrolia, hep-ph/0703311.
- [63] G. Ossola, C. G. Papadopoulos and R. Pittau, 0704.1271 [hep-ph].
- [64] Z. Bern, L. J. Dixon and D. A. Kosower, Nucl. Phys. B **513**, 3 (1998) [hep-ph/9708239].
- [65] L. D. Landau, Nucl. Phys. **13**, 181 (1959);
S. Mandelstam, Phys. Rev. **112**, 1344 (1958); Phys. Rev. **115**, 1741 (1959).
- [66] W. L. van Neerven, Nucl. Phys. B **268**, 453 (1986).
- [67] Z. Bern, L. J. Dixon and D. A. Kosower, JHEP **0408**, 012 (2004) [hep-ph/0404293].
- [68] Z. Bern, V. Del Duca, L. J. Dixon and D. A. Kosower, Phys. Rev. D **71**, 045006 (2005) [hep-th/0410224].
- [69] D. Forde, 0704.1835 [hep-ph].
- [70] A. Brandhuber, S. McNamara, B. J. Spence and G. Travaglini, JHEP **0510**, 011 (2005) [hep-th/0506068].
- [71] Z. Bern, L. J. Dixon and D. A. Kosower, Ann. Rev. Nucl. Part. Sci. **46**, 109 (1996) [hep-ph/9602280].
- [72] A. Brandhuber, B. Spence, G. Travaglini and K. Zoubos, 0704.0245 [hep-th].
- [73] F. Cachazo and P. Svrček, PoS **RTN2005**, 004 (2005) [hep-th/0504194].
- [74] L. J. Dixon, PoS **HEP2005**, 405 (2006) [hep-ph/0512111].
- [75] C. Schwinn and S. Weinzierl, JHEP **0704**, 072 (2007) [hep-ph/0703021].
- [76] Z. Bern, M. Czakon, L. J. Dixon, D. A. Kosower and V. A. Smirnov, Phys. Rev. D **75**, 085010 (2007) [hep-th/0610248];
Z. Bern, L. J. Dixon and R. Roiban, Phys. Lett. B **644**, 265 (2007) [hep-th/0611086];
Z. Bern, J. J. Carrasco, L. J. Dixon, H. Johansson, D. A. Kosower and R. Roiban, Phys. Rev. Lett. **98**, 161303 (2007) [hep-th/0702112].
- [77] F. A. Berends, R. Kleiss, P. De Causmaecker, R. Gastmans and T. T. Wu, Phys. Lett. B **103**, 124 (1981);
P. De Causmaecker, R. Gastmans, W. Troost and T. T. Wu, Nucl. Phys. B **206**, 53 (1982);
Z. Xu, D. H. Zhang and L. Chang, TUTP-84/3-TSINGHUA;
R. Kleiss and W. J. Stirling, Nucl. Phys. B **262**, 235 (1985);
J. F. Gunion and Z. Kunszt, Phys. Lett. B **161**, 333 (1985);
Z. Xu, D. H. Zhang and L. Chang, Nucl. Phys. B **291**, 392 (1987).
- [78] M. L. Mangano and S. J. Parke, Phys. Rept. **200**, 301 (1991);
L. J. Dixon, in *QCD & Beyond: Proceedings of TASI '95*, ed. D. E. Soper (World Scientific, 1996) [hep-ph/9601359].
- [79] J. E. Paton and H. M. Chan, Nucl. Phys. B **10**, 516 (1969);
P. Cvitanović, P. G. Lauwers and P. N. Scharbach, Nucl. Phys. B **186**, 165 (1981);
D. Kosower, B. H. Lee and V. P. Nair, Phys. Lett. B **201**, 85 (1988).
- [80] Z. Bern and D. A. Kosower, Nucl. Phys. B **362**, 389 (1991).
- [81] Z. Bern, L. J. Dixon and D. A. Kosower, Nucl. Phys. B **437**, 259 (1995) [hep-ph/9409393].
- [82] E. Witten, Commun. Math. Phys. **252**, 189 (2004) [hep-th/0312171].
- [83] R. Penrose, J. Math. Phys. **8**, 345 (1967).
- [84] M. H. Goroff and A. Sagnotti, Phys. Lett. B **160**, 81 (1985);
Nucl. Phys. B **266**, 709 (1986).
- [85] S. J. Parke and T. R. Taylor, Phys. Rev. Lett. **56**, 2459 (1986).
- [86] F. A. Berends and W. Giele, Nucl. Phys. B **294**, 700 (1987).
- [87] M. L. Mangano, S. J. Parke and Z. Xu, Nucl. Phys. B **298**, 653 (1988).
- [88] S. D. Badger, E. W. N. Glover, V. V. Khoze and P. Svrček, JHEP **0507**, 025 (2005) [hep-th/0504159].
- [89] R. Roiban, M. Spradlin and A. Volovich, Phys. Rev. Lett. **94**, 102002 (2005) [hep-th/0412265].

- [90] R. Britto, B. Feng, R. Roiban, M. Spradlin and A. Volovich, Phys. Rev. D **71**, 105017 (2005) [hep-th/0503198].
- [91] M. Dinsdale, M. Ternick and S. Weinzierl, JHEP **0603**, 056 (2006) [hep-ph/0602204].
- [92] K. Risager, JHEP **0512**, 003 (2005) [hep-th/0508206].
- [93] F. Cachazo, P. Svrček and E. Witten, JHEP **0409**, 006 (2004) [hep-th/0403047].
- [94] M. Luo and C. Wen, JHEP **0503**, 004 (2005) [hep-th/0501121]; Phys. Rev. D **71**, 091501 (2005) [hep-th/0502009];
D. de Florian and J. Zurita, JHEP **0611**, 080 (2006) [hep-ph/0609099]; JHEP **0605**, 073 (2006) [hep-ph/0605291].
- [95] S. D. Badger, E. W. N. Glover and V. V. Khoze, JHEP **0601**, 066 (2006) [hep-th/0507161];
D. Forde and D. A. Kosower, Phys. Rev. D **73**, 065007 (2006) [hep-th/0507292];
K. J. Ozeren and W. J. Stirling, Eur. Phys. J. C **48**, 159 (2006) [hep-ph/0603071];
C. F. Berger, V. Del Duca and L. J. Dixon, Phys. Rev. D **74**, 094021 (2006) [hep-ph/0608180].
- [96] K. J. Ozeren and W. J. Stirling, JHEP **0511**, 016 (2005) [hep-th/0509063].
- [97] L. M. Brown and R. P. Feynman, Phys. Rev. **85** (1952) 231;
L. M. Brown, Nuovo Cim. **21**, 3878 (1961).
- [98] G. Passarino and M. J. G. Veltman, Nucl. Phys. B **160**, 151 (1979).
- [99] W. L. van Neerven and J. A. M. Vermaseren, Phys. Lett. B **137**, 241 (1984);
G. J. van Oldenborgh and J. A. M. Vermaseren, Z. Phys. C **46**, 425 (1990).
- [100] R. Pittau, Comput. Phys. Commun. **104**, 23 (1997) [hep-ph/9607309]; Comput. Phys. Commun. **111**, 48 (1998) [hep-ph/9712418].
- [101] S. Weinzierl, Phys. Lett. B **450**, 234 (1999) [hep-ph/9811365].
- [102] Z. Bern and D. A. Kosower, Nucl. Phys. B **379**, 451 (1992).
- [103] Z. Bern, A. De Freitas, L. J. Dixon and H. L. Wong, Phys. Rev. D **66**, 085002 (2002) [hep-ph/0202271].
- [104] D. B. Melrose, Nuovo Cim. **40**, 181 (1965).
- [105] Z. Bern, L. J. Dixon and D. A. Kosower, Phys. Lett. B **302**, 299 (1993) [Erratum-ibid. B **318**, 649 (1993)] [hep-ph/9212308];
Z. Bern, L. J. Dixon and D. A. Kosower, Nucl. Phys. B **412**, 751 (1994) [hep-ph/9306240].
- [106] J. Fleischer, F. Jegerlehner and O. V. Tarasov, Nucl. Phys. B **566**, 423 (2000) [hep-ph/9907327];
T. Binoth, J. P. Guillet and G. Heinrich, Nucl. Phys. B **572**, 361 (2000) [hep-ph/9911342];
G. Duplancić and B. Nizić, Eur. Phys. J. C **35**, 105 (2004) [hep-ph/0303184].
- [107] R. E. Cutkosky, J. Math. Phys. **1**, 429 (1960).
- [108] R. J. Eden, P. V. Landshoff, D. I. Olive, J. C. Polkinghorne, *The Analytic S Matrix* (Cambridge University Press, 1966).
- [109] F. Cachazo, P. Svrček and E. Witten, JHEP **0410**, 077 (2004) [hep-th/0409245].
- [110] Z. Bern, N. E. J. Bjerrum-Bohr, D. C. Dunbar and H. Ita, JHEP **0511**, 027 (2005) [hep-ph/0507019].
- [111] J. M. Campbell, E. W. N. Glover and D. J. Miller, Nucl. Phys. B **498**, 397 (1997) [hep-ph/9612413].
- [112] Z. Bern and G. Chalmers, Nucl. Phys. B **447**, 465 (1995) [hep-ph/9503236].
- [113] Z. Bern, V. Del Duca and C. R. Schmidt, Phys. Lett. B **445**, 168 (1998) [hep-ph/9810409];
Z. Bern, V. Del Duca, W. B. Kilgore and C. R. Schmidt, Phys. Rev. D **60**, 116001 (1999) [hep-ph/9903516];
D. A. Kosower and P. Uwer, Nucl. Phys. B **563**, 477 (1999) [hep-ph/9903515];
S. D. Badger and E. W. N. Glover, JHEP **0407**, 040 (2004) [hep-ph/0405236].
- [114] Z. Bern, L. J. Dixon and D. A. Kosower, Phys. Rev. Lett. **70**, 2677 (1993) [hep-ph/9302280].
- [115] J. M. Campbell, private communication.
- [116] L. J. Dixon and A. Signer, Phys. Rev. D **56**, 4031 (1997) [hep-ph/9706285].
- [117] D. Vaman and Y. P. Yao, JHEP **0604**, 030 (2006) [hep-th/0512031].
- [118] G. Chalmers and W. Siegel, Phys. Rev. D **59**, 045013 (1999) [hep-ph/9801220].
- [119] D. Binosi and L. Theussl, Comput. Phys. Commun. **161**, 76 (2004) [hep-ph/0309015].
- [120] J. A. M. Vermaseren, Comput. Phys. Commun. **83**, 45 (1994).